indicate that ROCK inhibitor can be safely applied for cell injection therapy.

ROCK Inhibitor Provides RCECs with Phenotype to Reconstruct Corneal Endothelium

At 3 hours after injection, RCECs injected with Y-27632 were found to be markedly adhered to the basement membrane of the corneal endothelium (Figure 3A), suggesting that Y-27632 altered the adhesion properties of the RCECs and up-regulated cell adhesion on the basement membrane *in vivo*. To ascertain the causal effect of the elevated cell adhesion by Y-27632 in the induction of a pathologically transparent cornea, the histological phenotype of a donor cornea treated with Y-27632 was elucidated using a flat-mount cornea. The expression of ZO-1 and Na^+/K^+-ATPase was evident in RCECs injected with Y-27632, yet it was absent in RCECs injected without Y-27632. RCECs injected with Y-27632 exhibited a monolayer hexagonal cell shape, whereas RCECs injected without Y-27632 exhibited the stratified fibroblastic phenotype. Consistent with the stratified fibroblastic phenotype of RCECs injected without Y-27632, α-SMA (a marker of fibroblastic change) was evident in those RCECs (Figure 3B).

The existence of reconstructed corneal endothelium by the injection of RCECs with Y-27632 that expressed DiI, which labels RCECs, indicated that the injected RCECs contributed to the formation of a monolayer of corneal endothelium and to the inducement of corneal transparency (Figure 3B). However, DiI-expressing cells were also observed in the rabbits injected with RCECs without Y-27632, consistent with the results shown in Figure 1C. The presence of DiI-positive cells in the eyes injected with RCECs without Y-27632 may suggest that a limited number of RCECs were able to adhere to the cornea without the assistance of Y-27632, yet changed their phenotype to that of fibroblastic cells. This finding is consistent with those observed in the clinical setting, in which CECs display a fibroblastic phenotype in cases of corneal endothelial dysfunction.[22,23]

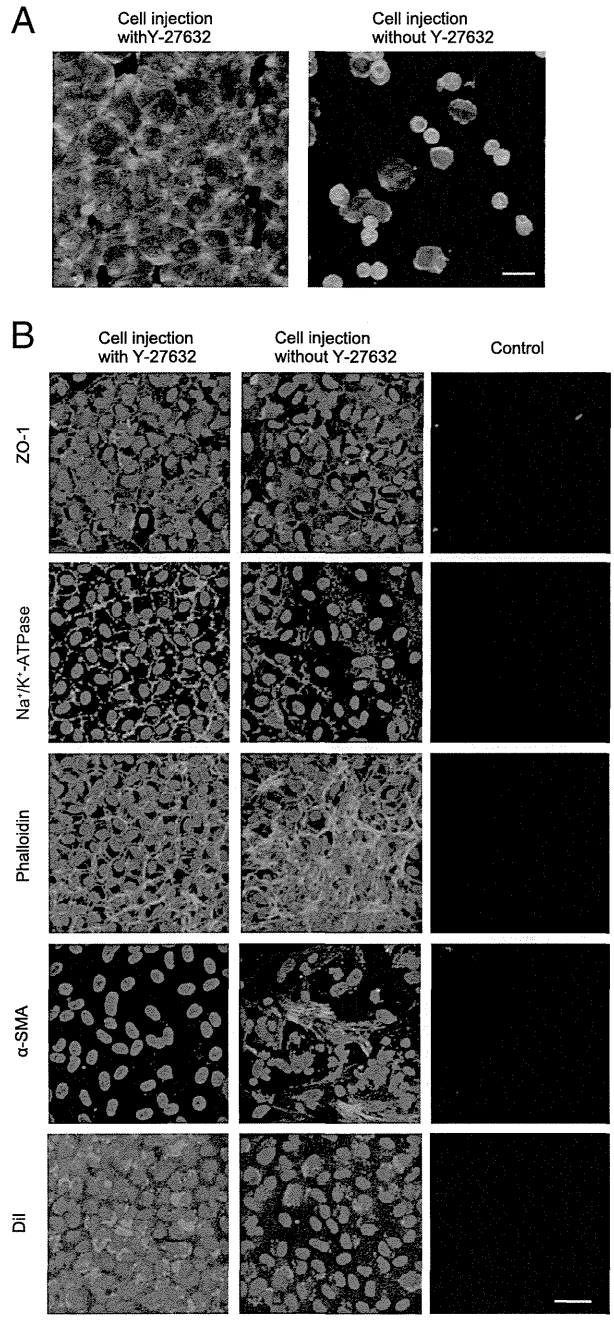

Figure 3. Histological examination of the reconstructed corneal tissue in rabbits after RCEC injection with and without Y-27632. **A:** Flat-mount examination of the posterior side of the corneal tissue 3 hours after RCEC injection. Green fluorescein shows actin-staining (phalloidin), and red shows nuclear staining by propidium iodide (PI). Scale bar = 100 μm. **B:** Histological examination of corneal tissue taken from the rabbit eye 2 weeks after RCEC injection with or without Y-27632. The histological phenotype of the injected RCECs was evaluated by immunofluorescence of ZO-1, Na^+/K^+-ATPase, phalloidin, α-SMA, and DiI after 2 weeks. No cells are observed in the control eyes in which the corneal endothelium was scraped. Scale bar = 100 μm.

ROCK Inhibitor Y-27632 Enhances Cell Adhesion

To examine the role of the Rho/ROCK signaling pathway in modulating the adhesion properties of primate CECs, cultivated MCECs were plated in combination with ROCK inhibitor Y-27632. Consistent with our previous findings,[20] phase contrast imaging and actin fiber staining revealed elevated cell adhesion in the Y-27632 treated cells (Figure 4A), and the cell adhesion was enhanced at the conventionally used concentration[24] (Figure 4B). MCECs treated with Y-27632 showed a markedly improved expression of vinculin in contrast to the non-treated cells (Figure 4C), suggesting that Y-27632 enhanced the cell adhesion via the induction of focal adhesion complexes. Considering the interplay between focal adhesion complex molecules and the extracellular matrix,[15] we next attempted to clarify the effect of Y-27632 on MCEC adhesion onto Descemet's membrane (basement membrane). Consistent with the *in vivo* experiments shown in Figure 3A, an *ex vivo* culture system

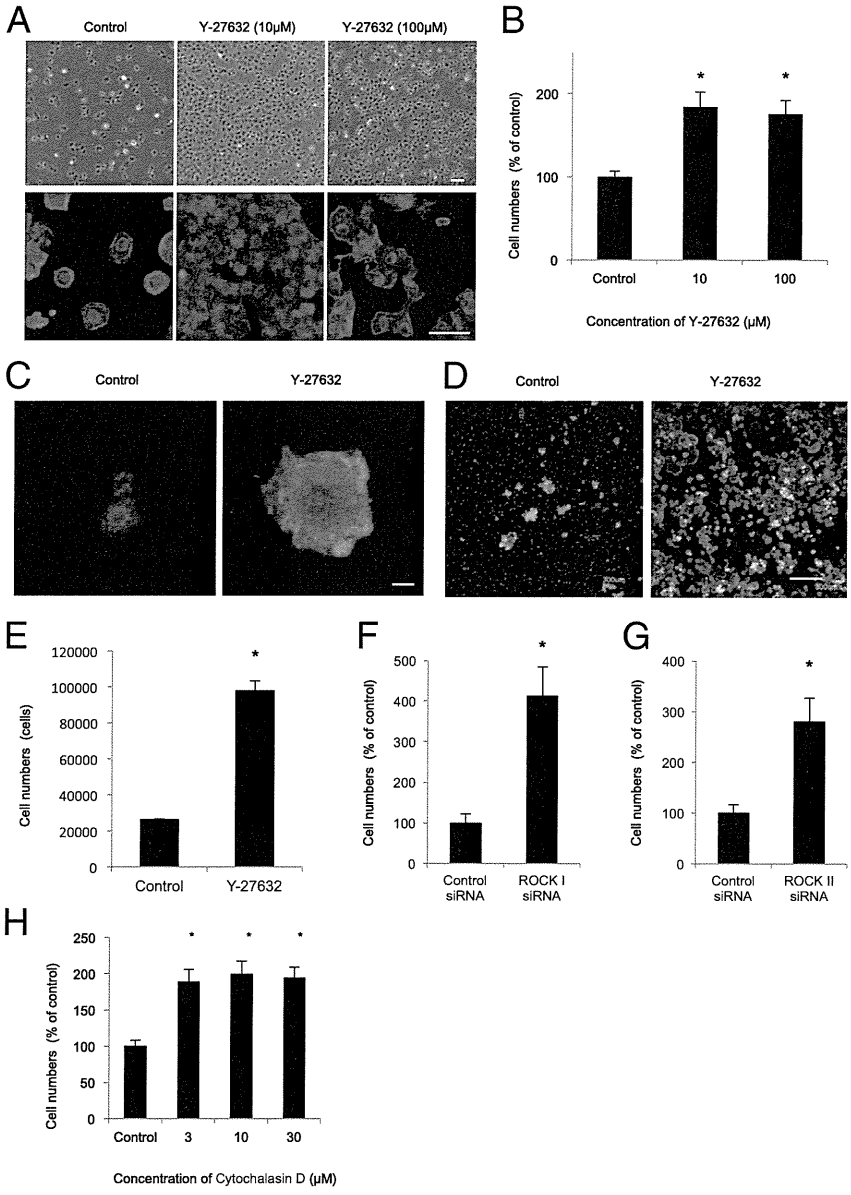

Figure 4. Rho/ROCK signaling pathway modulation of the adhesion properties of primate CECs in culture. **A:** Phase contrast images (**top row**) and actin fiber staining images (**bottom row**) reveal elevated cell adhesion in Y-27632–treated monkey CECs (MCECs) at 24 hours after seeding on a culture dish. Scale bar = 100 μm (**top row**), 50 μm (**bottom row**). **B:** The number of adhered MCECs is significantly enhanced by 10 μmol/L and 100 μmol/L of Y-27632 at 24 hours after seeding. Data are expressed as a percentage of the control, mean ± SEM. $*P < 0.01$. **C:** Representative immunofluorescence images of MCECs seeded with or without Y-27632 taken after staining with anti-vinculin at 3 hours after seeding. Scale bar = 10 μm. **D:** MCECs were seeded with or without Y-27632 on *ex vivo* culture system of rabbit Descemet's membrane and stained with actin antibody at 3 hours after seeding. Green fluorescein shows actin staining (phalloidin), and red shows nuclear staining by propidium iodide (PI). Scale bar = 300 μm. **E:** MCECs (density: 2.0×10^5 cells) were seeded with or without Y-27632 on rabbit Descemet's membrane, and the number of adhered cells was evaluated at 3 hours after seeding. Data are expressed as mean ± SEM. $*P < 0.01$. **F** and **G:** Direct contribution of the Rho/ROCK signaling pathway to the regulation of the adhesion properties of CECs was assessed by the knockdown of ROCK1 (**F**) or ROCK2 (**G**). Results are expressed as a percentage of the control, mean ± SEM. $*P < 0.01$. **H:** MCEC attachment was assessed through the inhibition of actin polymerization by cytochalasin D. Results are expressed as a percentage of the control, mean ± SEM. $*P < 0.01$.

demonstrated that Y-27632 dramatically enhanced the adhesion of the MCECs onto the basement membrane at 3 hours after seeding (Figure 4, D and E).

The direct contribution of the Rho/ROCK signaling pathway in elevating the adhesion properties was elucidated by the knockdown of ROCK I and ROCK II by RNAi (Figure 4, F and G; confirmed with three independent RNAi). Coincidentally, as with the elevated cell adhesion by Y-27632, the knockdown of both ROCK I and ROCK II strongly enhanced the cell adhesion. Because ROCK signaling is necessary to negatively regulate cell adhesion by inhibiting actin depolymerization, we speculate that inhibition of ROCK by Y-27632 promotes actin reorganization, subsequently inducing the enhancement of cell adhesion. In accordance with that speculation, we found that cytochalasin D, which is additionally capable of inhibiting actin polymerization, also elevated the MCEC adhesion (Figure 4H).

Injection of Cultivated CECs with ROCK Inhibitor Enables Regeneration of Cornea in a Primate Model

The injection of cultivated MCECs combined with Y-27632 was performed in a cynomolgus monkey in which the corneal endothelium was mechanically removed to produce a pathological dysfunction model. To elucidate the long-term efficacy of the injection of CECs with ROCK inhibitor Y-27632, that monkey model was observed for 3 months. In contrast to the rabbit model, slit-lamp microscopy showed that the monkey eyes injected with MCECs, both with and without Y-27632, exhibited complete corneal transparency within 1 week, and that the transparency persisted throughout 3 months of cell injection with a normal range of thickness (<600 μm) (Figure 5A). To evaluate the histological phenotype of donor corneas, two of four mon-

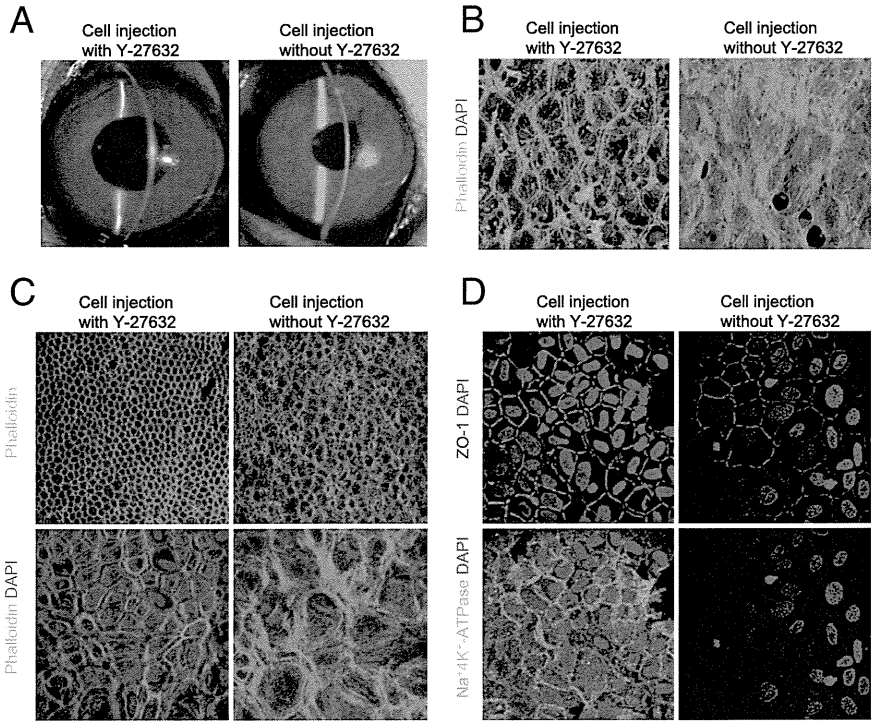

Figure 5. Regeneration of the cornea in a primate model enabled by the injection of cultivated MCECs with Y-27632. **A:** Monkey eyes injected with MCECs with Y-27632 or without Y-27632 exhibit a transparent cornea with a normal range of thickness (<600 μm) after 3 months. **B:** Histological analysis by actin immunostaining after 2 weeks of cell injection of MCECs injected with or without Y-27632. **C:** Histological analysis by actin immunostaining after 3 months of cell injection of MCECs injected with or without Y-27632. **Top row:** lower magnification (green, actin); **bottom row:** higher magnification (green, actin; blue, DAPI). The cell density of the MCECs injected without Y-27632 was 789 cells/mm^2, whereas that with Y-27632 was 2208 cells/mm^2. **D:** Histological analysis was performed after immunostaining of ZO-1 (red) or Na^+/K^+-ATPase (green). DAPI was used for nuclei staining (blue).

keys were euthanized after 2 weeks of MCEC injection and the other two monkeys after 3 months of MCEC injection (one monkey that received MCEC injection with Y-27632 and one monkey that received MCEC injection without Y-27632, respectively, at each of the two time points). It is notable that the MCECs injected with Y-27632 exhibited a monolayer cell shape, whereas the MCECs injected without Y-27632 exhibited a stratified fibroblastic phenotype at the 2-week time point, which mirrored the rabbit model findings (Figure 5B). Although slit-lamp microscopy showed that the monkey eyes injected with MCECs, both with and without Y-27632, exhibited a transparent cornea with a normal-range corneal thickness, MCECs injected without Y-27632 exhibited a fibroblastic phenotype at the cell density of 789 cells/mm^2, whereas MCECs injected with Y-27632 exhibited a monolayer hexagonal cell phenotype at the cell density of 2208 cells/mm^2 (Figure 5C), suggesting that Y-27632 also enhanced the adhesion of MCECs in the *in vivo* monkey model. Consistent with the rabbit experiments, the MCECs injected with Y-27632 expressed ZO-1 and Na^+/K^+-ATPase, yet they were expressed to a lesser degree in the MCECs injected without Y-27632 that exhibited the fibroblastic phenotype (Figure 5D).

Discussion

Corneal endothelial dysfunction accompanied by visual disturbance is a major indication for corneal transplantation surgery.[25] Although corneal transplantation is widely performed for corneal endothelial dysfunction, the transplantation of cultivated corneal endothelium is a potential therapeutic strategy. Cultivated CECs derived from older donors have lower proliferative ability, a senescent cell phenotype, and transformed cell morphology, thus suggesting less functional ability than those derived from younger donors.[26] When corneal endothelium is cultured and stocked as "master cells," it allows for the transplantation of CECs derived from younger donors, thus providing cells with high functional ability and an extended longevity. In addition, it enables an HLA-matching transplantation to reduce the risk of rejection[27,28] and to overcome the shortage of donor corneas. In the clinical setting, transplantation of corneal endothelium is technically difficult, because it is a monolayer and is located in the anterior chamber. Thus, that anatomical feature led us to hypothesize that the injection of cultivated CECs would be a potent therapy, even though a previous study reported that cell injection itself was ineffective.[12] The findings of this present study show that the inclusion of ROCK inhibitor Y-27632 elevates the adhesion property of CECs, thus allowing the successful transplantation of CECs to reconstruct functional corneal endothelium damaged by pathological dysfunctions.

We previously reported that the inhibition of ROCK by use of the selective ROCK inhibitor Y-27632 elevates the adhesion of cultured CECs on the substrate, enhances cell proliferation, and suppresses apoptosis.[20] Although the precise underlying mechanisms have yet to be elucidated, those distinct positive effects of ROCK inhibition enable the establishment of the *in vitro* expansion of CECs for cultivated corneal endothelial transplantation.[20] Rho–ROCK signaling carries out a variety of cellular processes such as cell adhesion, morphogenesis, migration, and cell-cycle progression through mediating cytoskeletal dynamics. The Rho GTPase-specific guanine nucleotide exchange factors (Rho GEFs) convert Rho from the guanosine diphosphate (GDP)–bound inactive form to

the guanosine triphosphate (GTP)–bound active form, thus inducing Rho GTPase activity. Rho regulates a variety of cytoskeletal dynamics that underlie cell morphology and adhesion through the activation of ROCK, a major downstream effector.[16,19] ROCK signaling modulates acto-myosin contractility through the regulation of myosin phosphorylation and actin dynamics by promoting nucleation and polymerization or by stimulating the severing and depolymerization of existing actin filaments.[17,29] It is reported that the actin cytoskeleton plays a critical role in regulating the adhesive property through interaction between the actin cytoskeleton and integrin.[14,17,18] Although the adhesive property is dependent on the cell type and the environmental context, ROCK signaling has been shown to negatively regulate the integrin adhesions of monocytes[17] and leukocytes.[18] Findings from a recent study showed that the RhoA–ROCK–PTEN pathway was highly activated when pre-osteoblasts are poorly attached to the substrate, and that the inhibition of this pathway enhances cell adhesion as well as proliferation.[30] Our findings that the inhibition of ROCK signaling by a selective ROCK inhibitor or by the siRNA enhanced adhesive property of CECs are consistent with the findings of those previous studies. Our findings are also supported by our data that inhibiting actin polymerization by cytochalasin D enhances the adhesive property. Furthermore, we found that vinculin, which is involved in the linkage of the integrin adhesion complex to the actin cytoskeleton,[31,32] is upregulated in ROCK-inhibitor-treated CECs. Further investigation is needed to elucidate whether the ROCK inhibitor promotes the focal adhesions through inhibiting actin polymerization and induces the upregulation of cell adhesion properties on the extracellular matrix (ECM).

Corneal endothelial dysfunctions such as Fuchs's endothelial corneal dystrophy, pseudoexfoliation syndrome, keratitis, and injury induce the fibroblastic transformation of CECs.[22,23] In addition, CECs reportedly showed fibroblastic transformation during the wound healing process,[33] and IL-1β–mediated FGF-2 produced after an injury reportedly alters CEC morphology and the actin cytoskeleton in a rabbit freezing injury model.[34] Our findings that RCECs without Y-27632 injected into the anterior chamber of a bullous keratopathy rabbit model exhibited stratified fibroblastic cell morphology and a resultant opaque cornea are consistent with these studies. On the other hand, MCECs without Y-27632 exhibited less fibroblastic phenotype. In our current primate model, a low density of MCECs compensated the pump and barrier functions and resulted in a clear cornea. That finding might possibly be explained by differences in the wound healing process between species.[35,36] However, because CEC density continuously decreases after keratoplasty,[37] reconstructed corneal endothelium with Y-27632 at a high cell density is crucial for the successful long-term outcome of transplantation in the clinical setting. To establish the application of a cultivated CEC injection combined with ROCK inhibitor in clinical settings, transplantation models more akin to humans are required, as rabbit CECs exhibit a high proliferative ability *in vivo*,[38] unlike human CECs. The findings from this present study demonstrated that a monkey eye injected with MCECs with Y-27632 exhibited an almost completely clear cornea. Thus, our primate model–based findings suggest that the cell injection therapy in which the cell adhesion is modulated by ROCK inhibitor might prove to be an effective treatment regimen for human corneal endothelial disorders.

In regard to future clinical applications, ROCK inhibitors have been shown to be useful for a wide range of diseases such as cardiovascular disease, pulmonary disease, cancer, and glaucoma.[21,39–41] Fasudil, one of the ROCK inhibitors, has already been used clinically for the prevention and treatment of cerebral vasospasm, and to date has been therapeutically applied in over 124,000 cases in Japan.[21] Furthermore, we previously demonstrated that a ROCK inhibitor eye drop enhanced corneal endothelial proliferation *in vitro*,[20] as well as in an *in vivo* animal model,[42] and it is currently under clinical research for corneal endothelial dysfunction. These facts suggest that the ROCK inhibitor is a therapeutic tool that can be safely and effectively applied in the clinical setting.

In conclusion, the findings of this present study, which are supported by both rabbit and primate corneal endothelial dysfunction models, indicate that ROCK inhibitor Y-27632 will enable the establishment of a cultivated-CEC–based therapy. Modulating actin cytoskeletal dynamics through Rho-ROCK signaling activity serves as a potential for cell-based regenerative medicine to enhance cell engraftment. This novel strategy of using a cell-based therapy combined with a ROCK inhibitor may ultimately provide clinicians with a new therapeutic modality in regenerative medicine, not only for the treatment of corneal endothelial dysfunctions but also for a variety of pathological diseases.

Acknowledgments

We thank Drs. Yoshiki Sasai and Masatoshi Ohgushi for assistance and invaluable advice regarding ROCK inhibitors, Takahiro Nakagawa for assistance with the monkey experiments, Kenta Yamasaki, Mayumi Yamamoto, Yuri Tsukahara, and Toshie Isobe for technical assistance, and John Bush for reviewing the manuscript.

References

1. Gorovoy MS: Descemet-stripping automated endothelial keratoplasty. Cornea 2006, 25:886–889
2. Price FW, Jr., Price MO: Descemet's stripping with endothelial keratoplasty in 50 eyes: a refractive neutral corneal transplant. J Refract Surg 2005, 21:339–345
3. Koizumi N, Sakamoto Y, Okumura N, Okahara N, Tsuchiya H, Torii R, Cooper LJ, Ban Y, Tanioka H, Kinoshita S: Cultivated corneal endothelial cell sheet transplantation in a primate model. Invest Ophthalmol Vis Sci 2007, 48:4519–4526
4. Koizumi N, Sakamoto Y, Okumura N, Tsuchiya H, Torii R, Cooper LJ, Ban Y, Tanioka H, Kinoshita S: Cultivated corneal endothelial transplantation in a primate: possible future clinical application in corneal endothelial regenerative medicine. Cornea 2008, 27 Suppl 1:S48–S55
5. Mimura T, Yamagami S, Yokoo S, Usui T, Tanaka K, Hattori S, Irie S, Miyata K, Araie M, Amano S: Cultured human corneal endothelial cell

transplantation with a collagen sheet in a rabbit model. Invest Ophthalmol Vis Sci 2004, 45:2992–2997
6. Ishino Y, Sano Y, Nakamura T, Connon CJ, Rigby H, Fullwood NJ, Kinoshita S: Amniotic membrane as a carrier for cultivated human corneal endothelial cell transplantation. Invest Ophthalmol Vis Sci 2004, 45:800–806
7. Schachinger V, Erbs S, Elsasser A, Haberbosch W, Hambrecht R, Holschermann H, Yu J, Corti R, Mathey DG, Hamm CW, Suselbeck T, Assmus B, Tonn T, Dimmeler S, Zeiher AM: Intracoronary bone marrow-derived progenitor cells in acute myocardial infarction. N Engl J Med 2006, 355:1210–1221
8. Tateishi-Yuyama E, Matsubara H, Murohara T, Ikeda U, Shintani S, Masaki H, Amano K, Kishimoto Y, Yoshimoto K, Akashi H, Shimada K, Iwasaka T, Imaizumi T: Therapeutic angiogenesis for patients with limb ischaemia by autologous transplantation of bone-marrow cells: a pilot study and a randomised controlled trial. Lancet 2002, 360:427–435
9. Shapiro AM, Lakey JR, Ryan EA, Korbutt GS, Toth E, Warnock GL, Kneteman NM, Rajotte RV: Islet transplantation in seven patients with type 1 diabetes mellitus using a glucocorticoid-free immunosuppressive regimen. N Engl J Med 2000, 343:230–238
10. Yanaga H, Koga M, Imai K, Yanaga K: Clinical application of biotechnically cultured autologous chondrocytes as novel graft material for nasal augmentation. Aesthetic Plast Surg 2004, 28:212–221
11. Mimura T, Shimomura N, Usui T, Noda Y, Kaji Y, Yamgami S, Amano S, Miyata K, Araie M: Magnetic attraction of iron-endocytosed corneal endothelial cells to Descemet's membrane. Exp Eye Res 2003, 76: 745–751
12. Mimura T, Yamagami S, Usui T, Ishii Y, Ono K, Yokoo S, Funatsu H, Araie M, Amano S: Long-term outcome of iron-endocytosing cultured corneal endothelial cell transplantation with magnetic attraction. Exp Eye Res 2005, 80:149–157
13. Patel SV, Bachman LA, Hann CR, Bahler CK, Fautsch MP: Human corneal endothelial cell transplantation in a human ex vivo model. Invest Ophthalmol Vis Sci 2009, 50:2123–2131
14. Sastry SK, Burridge K: Focal adhesions: a nexus for intracellular signaling and cytoskeletal dynamics. Exp Cell Res 2000, 261:25–36
15. Critchley DR: Focal adhesions—the cytoskeletal connection. Curr Opin Cell Biol 2000, 12:133–139
16. Hall A: Rho GTPases and the actin cytoskeleton. Science 1998, 279:509–514
17. Worthylake RA, Lemoine S, Watson JM, Burridge K: RhoA is required for monocyte tail retraction during transendothelial migration. J Cell Biol 2001, 154:147–160
18. Worthylake RA, Burridge K: RhoA and ROCK promote migration by limiting membrane protrusions. J Biol Chem 2003, 278:13578–13584
19. Narumiya S, Tanji M, Ishizaki T: Rho signaling, ROCK and mDia1, in transformation, metastasis and invasion. Cancer Metastasis Rev 2009, 28:65–76
20. Okumura N, Ueno M, Koizumi N, Sakamoto Y, Hirata K, Hamuro J, Kinoshita S: Enhancement on primate corneal endothelial cell survival in vitro by a ROCK inhibitor. Invest Ophthalmol Vis Sci 2009, 50: 3680–3687
21. Liao JK, Seto M, Noma K: Rho kinase (ROCK) inhibitors. J Cardiovasc Pharmacol 2007, 50:17–24
22. Naumann GO, Schlotzer-Schrehardt U: Keratopathy in pseudoexfoliation syndrome as a cause of corneal endothelial decompensation: a clinicopathologic study. Ophthalmology 2000, 107:1111–1124
23. Kawaguchi R, Saika S, Wakayama M, Ooshima A, Ohnishi Y, Yabe H: Extracellular matrix components in a case of retrocorneal membrane associated with syphilitic interstitial keratitis. Cornea 2001, 20:100–103
24. Narumiya S, Ishizaki T, Uehata M: Use and properties of ROCK-specific inhibitor Y-27632. Methods Enzymol 2000, 325:273–284
25. Darlington JK, Adrean SD, Schwab IR: Trends of penetrating keratoplasty in the United States from 1980 to 2004. Ophthalmology 2006, 113:2171–2175
26. Joyce NC, Zhu CC: Human corneal endothelial cell proliferation: potential for use in regenerative medicine. Cornea 2004, 23:S8–S19
27. Khaireddin R, Wachtlin J, Hopfenmuller W, Hoffmann F: HLA-A. HLA-B and HLA-DR matching reduces the rate of corneal allograft rejection. Graefes Arch Clin Exp Ophthalmol 2003, 241:1020–1028
28. Coster DJ, Williams KA: The impact of corneal allograft rejection on the long-term outcome of corneal transplantation. Am J Ophthalmol 2005, 140:1112–1122
29. Ishizaki T, Uehata M, Tamechika I, Keel J, Nonomura K, Maekawa M, Narumiya S: Pharmacological properties of Y-27632, a specific inhibitor of rho-associated kinases. Mol Pharmacol 2000, 57:976–983
30. Yang S, Kim HM: The RhoA-ROCK-PTEN pathway as a molecular switch for anchorage dependent cell behavior. Biomaterials 2012, 33:2902–2915
31. Geiger B: A 130K protein from chicken gizzard: its localization at the termini of microfilament bundles in cultured chicken cells. Cell 1979, 18:193–205
32. Burridge K, Feramisco JR: Microinjection and localization of a 130K protein in living fibroblasts: a relationship to actin and fibronectin. Cell 1980, 19:587–595
33. Ichijima H, Petroll WM, Jester JV, Barry PA, Andrews PM, Dai M, Cavanagh HD: In vivo confocal microscopic studies of endothelial wound healing in rabbit cornea. Cornea 1993, 12:369–378
34. Lee HT, Lee JG, Na M, Kay EP: FGF-2 induced by interleukin-1 beta through the action of phosphatidylinositol 3-kinase mediates endothelial mesenchymal transformation in corneal endothelial cells. J Biol Chem 2004, 279:32325–32332
35. Matsubara M, Tanishima T: Wound-healing of the corneal endothelium in the monkey: a morphometric study. Jpn J Ophthalmol 1982, 26:264–273
36. Matsubara M, Tanishima T: Wound-healing of corneal endothelium in monkey: an autoradiographic study. Jpn J Ophthalmol 1983, 27:444–450
37. Bourne WM, Nelson LR, Hodge DO: Central corneal endothelial cell changes over a ten-year period. Invest Ophthalmol Vis Sci 1997, 38:779–782
38. Van Horn DL, Sendele DD, Seideman S, Buco PJ: Regenerative capacity of the corneal endothelium in rabbit and cat. Invest Ophthalmol Vis Sci 1977, 16:597–613
39. Koga T, Awai M, Tsutsui J, Yue BY, Tanihara H: Rho-associated protein kinase inhibitor, Y-27632, induces alterations in adhesion, contraction and motility in cultured human trabecular meshwork cells. Exp Eye Res 2006, 82:362–370
40. Olson MF: Applications for ROCK kinase inhibition. Curr Opin Cell Biol 2008, 20:242–248
41. Tokushige H, Inatani M, Nemoto S, Sakaki H, Katayama K, Uehata M, Tanihara H: Effects of topical administration of y-39983, a selective rho-associated protein kinase inhibitor, on ocular tissues in rabbits and monkeys. Invest Ophthalmol Vis Sci 2007, 48:3216–3222
42. Okumura N, Koizumi N, Ueno M, Sakamoto Y, Takahashi H, Hirata K, Torii R, Hamuro J, Kinoshita S: Enhancement of corneal endothelium wound healing by Rho-associated kinase (ROCK) inhibitor eye drops. Br J Ophthalmol 2011, 95:1006–1009

Simultaneous Analysis of Multiple Cytokines in the Vitreous of Patients with Sarcoid Uveitis

Kenji Nagata,[1] *Kazuichi Maruyama,*[1] *Kazuko Uno,*[2] *Katsuhiko Shinomiya,*[1] *Kazuhito Yoneda,*[1] *Junji Hamuro,*[1] *Sunao Sugita,*[3] *Takeru Yoshimura,*[4] *Koh-Hei Sonoda,*[5] *Manabu Mochizuki,*[3] *and Shigeru Kinoshita*[1]

Purpose. Levels of some cytokines are significantly higher in the vitreous fluid of patients with acute uveitis than in normal vitreous fluid. The authors sought to determine which proinflammatory cytokines were upregulated in the vitreous fluid of patients with ocular sarcoidosis.

Methods. Samples of vitreous fluid were collected from patients with sarcoid uveitis and from nonsarcoid control patients with idiopathic epiretinal membrane. The levels of 27 proinflammatory cytokines were measured with a multiplex beads array system. Postvitrectomy macular thickness was also measured by using spectral domain optical coherence tomography (SD-OCT). To assess the relationship between cytokine levels and disease stage, the authors divided patients into three groups based on macular thickness 1 month after operation.

Results. The vitreous levels of 17 cytokines were significantly higher in patients with ocular sarcoidosis than in nonsarcoid controls. Serum levels of interferon γ-induced protein 10 (IP-10) were also higher in ocular sarcoidosis patients than in nonsarcoid controls. Conversely, serum levels of interleukin (IL) 15 in ocular sarcoidosis patients were lower than in the control group. Analysis of cytokine levels and macular thickness revealed that IL-1ra, IL-4, IL-8, IFN-γ, IP-10, monocyte chemotactic protein (MCP)-1, macrophage inflammatory protein (MIP)-1β, and regulated on activation, normal T-cell expressed and secreted (RANTES) were significantly upregulated in patients with thin cystoid macular edema group.

Conclusions. Patients with ocular sarcoidosis had elevated levels of proinflammatory cytokines in vitreous fluids. Different cytokines might contribute to different stages of macular edema. (*Invest Ophthalmol Vis Sci.* 2012;53:3827–3833) DOI: 10.1167/iovs.11-9244

From the [1]Department of Ophthalmology, Kyoto Prefectural University of Medicine, Kyoto, Japan; the [2]Louis Pasteur Center for Medical Research, Kyoto, Japan; the [3]Department of Ophthalmology, Tokyo Dental and Medical University, Tokyo, Japan; the [4]Department of Ophthalmology, Graduate School of Medical Science, Kyushu University, Fukuoka, Japan; and the [5]Department of Ophthalmology, Yamaguchi University Graduate School of Medicine, Yamaguchi, Japan.

Supported by KAKEN 22791679 and KAKEN 10433244.

Submitted for publication December 5, 2011; revised March 30 and April 28, 2012; accepted May 4, 2012.

Disclosure: **K. Nagata**, None; **K. Maruyama**, None; **K. Uno**, None; **K. Shinomiya**, None; **K. Yoneda**, None; **J. Hamuro**, None; **S. Sugita**, None; **T. Yoshimura**, None; **K.-H. Sonoda**, None; **M. Mochizuki**, None; **S. Kinoshita**, None

Corresponding author: Kazuichi Maruyama, Department of Ophthalmology, Kyoto Prefectural University of Medicine, 465 Kajii-cho, Hirokoji-agaru, Kawaramachi-dori, Kamigyo-ku, Kyoto 602-0841, Japan; kmaruyam@koto.kpu-m.ac.jp.

Sarcoidosis is a chronic multisystem granulomatous disorder of unknown etiology.[1–4] It is thought to result from an exaggerated cellular immune response to a variety of self-antigens or nonself antigens.[5] The lung is the organ most frequently affected by this disease, and when affected, it is characterized by bilateral hilar lymphadenopathy and/or pulmonary infiltration as revealed by chest radiography. Ocular and skin lesions are also common aspects of sarcoidosis, but other organs (including the heart, the central nervous system, and the spleen) may also be affected.[6] Although the exact cause of sarcoidosis is currently unknown, previous reports have discussed environmental (e.g., spatial[7] or climatic[8]) factors, occupational factors, or infectious agents (specifically, propionibacteria[9–11]) as possible causes.

Reportedly, 30% to 60% of patients with sarcoidosis suffer from ocular involvement.[12–15] Bilateral anterior and/or posterior uveitis is common, but the conjunctiva, lacrimal gland, and orbit of the eye can also be affected. The clinical presentation of sarcoidosis-related uveitis is characteristically marked by iris nodules, mutton-fat keratic precipitates, and tent-shaped peripheral anterior synechia in the anterior segment of the eye. Snowball-like vitreous opacity, which results from phlebitis and vitreitis, is a common posterior segment finding. Chronic uveitis can result in formation of an epiretinal membrane (ERM) and cystoid macular edema (CME); consequently, severe visual impairment can occur.[16] Uveitis is commonly treated with topical (or occasionally systemic) administration of corticosteroids, but in cases accompanied by the formation of an ERM or long-standing vitreous opacity, surgical treatment is necessary.

An internationally acknowledged set of criteria for the diagnosis of ocular sarcoidosis has been established.[17] Previously, it has been reported that the types of cytokines in ocular fluids are dependent on the disease.[18,19] The authors thus sought to assess vitreous cytokine levels and correlate them with disease status in ocular sarcoidosis. The multiplex bead analysis system is a new technique that combines the principle of the sandwich immunoassay with fluorescent bead-based technology. Levels of many types of cytokines in small sample volumes (such as vitreous samples) can be measured simultaneously with this system. Sato et al.[20] have used this method to show that the levels of vascular endothelial growth factor A (VEGF-A) are much higher than those of any type of cytokine in infants with retinopathy of prematurity (ROP). There are also several reports about the levels of various cytokines in vitreous fluid from uveitis patients.[21–25] Yoshimura et al.[18] reported that interleukin (IL) 6, IL-8, and monocyte chemotactic protein-1 (MCP-1) were elevated in the vitreous body of patients with diabetic retinopathy and retinal vein occlusion.

Analyses of many cytokines in peripheral blood or bronchoalveolar lavage fluid (BALF) have elucidated the

pathogenesis of sarcoidosis. For example, high amounts of interferon γ-induced protein 10 (IP-10) are secreted from sarcoid-dependent alveolar macrophages and T cells.[26] However, to the authors' knowledge, investigations of cytokine levels in both vitreous fluid and serum from patients with sarcoid uveitis have not been conducted with multiplex bead analysis.

Here, the vitreous and serum levels of 27 types of cytokines in patients with sarcoid uveitis were measured and compared with those from patients with idiopathic ERM. Moreover, the authors investigated the relationship between vitreous cytokine levels and CME severity.

METHODS

Patients

This study was performed in accordance with the tenets of the Declaration of Helsinki, and the procedures were approved by the Institutional Review Board of the Kyoto Prefectural University of Medicine Hospital. Twenty-one patients gave informed consent for participation in this study.

For the multiplex bead analysis of vitreous fluid, a total of 24 samples were enrolled. Of the 20 patients, 15 (1 man and 14 women) had diagnoses of ocular sarcoidosis for one or both eyes (19 eyes total), based on the international criteria. Vitreous fluid was collected from five eyes of five idiopathic ERM patients (3 men and 2 women), who were enrolled as nonsarcoid controls.

General examinations of all patients were performed by using the algorithm designed for the diagnosis of ocular sarcoidosis.[17]

The group of patients with ocular sarcoidosis comprised 1 man and 14 women; the idiopathic ERM (nonsarcoid control) group comprised 2 men and 3 women. The mean age of the ocular sarcoidosis patients was 66.8 ± 2.2 years, and that of the idiopathic ERM patients was 69.5 ± 3.1 years. Statistical differences were not found in mean age.

Vitreous Sample Collection

Vitreous specimens were obtained from each of 20 patients at the start of a conventional 25-gauge pars plana vitrectomy by using either a CV-24,000 (NIDEK Co., Ltd., Aichi, Japan) or an Accurus (Alcon Laboratories, Inc., Fort Worth, TX) vitrectomy system. A three-way stopcock was attached to the connector on the suction-tube line of the cutter probe, and a 5-ml syringe was connected to the free end of the three-way stopcock. Dry vitrectomy without perfusion of balanced salt solution (Alcon Laboratories, Inc.) was conducted with a cut rate of 500 cpm so as not to damage cells infiltrating into the vitreous. At least 500 μL dry vitreous sample was collected from each patient. Each sample was divided into 5 microtubes for each analysis (200 μL for PCR, 200 μL for multiplex bead analysis, and 100 μL for culture). No intraoperative complications occurred in these patients.

Multiplex Bead Analysis System (Multiplex-ELISA)

The vitreous levels of 27 types of cytokines were determined by using a commercially available multiplex bead analysis system (BioPlex Pro Suspension Array System; BioRad Laboratories, Tokyo, Japan). The 27 cytokines measured were IL-1b; IL-1 receptor antagonist (IL-1ra); IL-2; IL-4; IL-5; IL-6; IL-7; IL-8; IL-9; IL-10; IL-12; IL-13; IL-15; IL-17; eotaxin; basic fibroblast growth factor (bFGF); granulocyte colony-stimulating factor (G-CSF); granulocyte macrophage colony-stimulating factor (GM-CSF); IFN-γ; IFN-γ–IP-10; MCP-1; macrophage inflammatory protein (MIP)-1α and MIP-1β platelet-derived growth factor BB (PDGF-BB); regulated on activation, normal T-cell expressed and secreted (RANTES); tumor necrosis factor α (TNF-α); and VEGF.

Multiplex PCR

Human herpes virus (HHV) genomic DNA was assayed in vitreous fluids by using two independent PCR assays (a qualitative multiplex PCR assay and a quantitative real-time PCR assay) as described previously.[27,28] DNA was extracted from samples by using an E21 virus minikit (QIAGEN, Inc., Valencia, CA) installed on a robotic workstation for automated purification of nucleic acids (BioRobot E21; QIAGEN). Multiplex PCR was designed to qualitatively identify the genomic DNA of the following 8 types of HHV: herpes simplex virus type 1 (HSV-1 or HHV-1) and type 2 (HSV-2 or HHV-2), varicella zoster virus (VZV or HHV-3), Epstein-Barr virus (EBV or HHV-4), cytomegalovirus (CMV or HHV-5), HHV6, HHV7, and HHV8. Other ocular pathogens were also tested, such as *Propionibacterium acnes*, *Toxoplasma*, *Toxocara*, *Bartonella henselae*, *Chlamydia trachomatis*, *Treponema pallidum*, *Mycobacterium tuberculosis*, *Candida* (18s rRNA), *Aspergillus* (18s rRNA), and bacterial 16s rRNA. PCR was performed with a LightCycler (Roche Diagnostics [Schweiz] AG, Rotkreuz, Switzerland). Primers and probes used to detect HHV1 to HHV8 and the PCR conditions have all been described previously.[27] Specific primers for each virus were used with Accuprime *Taq* (Invitrogen, Carlsbad, CA). The templates were subjected to 40 cycles of PCR amplification, and probes were then mixed with the PCR products. Subsequently, real-time PCR was performed only for the HHVs, with the genomic DNA detected by multiplex PCR. The real-time PCR was performed with AmpliTaq Gold (Applied Biosystems, Foster City, CA) and the Real-Time PCR 7300 system (Applied Biosystems). All of the templates obtained were subjected to 45 cycles of PCR amplification. The value of the viral copy number in the sample was considered to be significant when more than 50 copies per tube (5×10^3 copies/mL) were observed.

Macular Thickness Measurement in Ocular Sarcoidosis Patients

The patients who received surgical intervention and cytokine measurements were also evaluated for macular thickness. Macular 3D scans with the spectral-domain 3D-OCT 1000 (TOPCON, Itabashi, Japan) were performed at 1 month after surgery. Patients were divided into two groups on the basis of macular thickness, which was calculated as the average thickness of macular area (fovea 1000 μm across) ± SD. The thin CME range (group 1; 10 patients and 12 eyes) was 119.60 μm to 359.5 μm, and the thick CME range (group 2; 9 patients and 10 eyes) was 359.5 μm to 599.40 μm. Some patients overlapped because of different status of disease in each eye.

Statistical Analysis

Statistical comparisons of the cytokine concentrations of the two patient groups (sarcoidosis and ERM) were carried out by nonparametric analysis with the Mann-Whitney *U* test. The statistical evaluation of the data was performed by using Bonferroni correction. A P value <0.025 was considered to be statistically significant. Statistical comparisons of the macular thickness of three groups (CME grade) were carried out by nonparametric analysis with the Mann-Whitney *U* test.

RESULTS

Vitreous and Serum Levels of 27 Types of Cytokines

The vitreous and serum levels of cytokines are shown in Tables 1 and 2. The levels of PDGF-BB, IL-1ra, IL-4, IL-5, IL-6, IL-8, IL-9, IL-10, IL-12, G-CSF, IFN-γ, IP-10, MCP-1α, MIP-1β, RANTES, TNF-α, and VEGF were significantly higher in the vitreous from patients with ocular sarcoidosis than in that of ERM (non-

Table 1. Vitreous Fluid Levels of 27 Types of Cytokines Determined by Using a Multiplex Bead Analysis System

	Sarcoidosis Vitreous, Mean ± SE ($N = 19$)	ERM Vitreous, Mean ± SE ($N = 5$)	*P* Value
PDGF-BB	74.54 ± 12.89	1.29 ± 0.81	0.0043*
IL-1β	0.60 ± 0.08	1.07 ± 0.78	0.1766
IL-1ra	225.1 ± 69.88	7.93 ± 1.76	0.0008†
IL-2	0.885 ± 0.36	0	0.2526
IL-4	0.67 ± 0.09	0.02 ± 0.02	0.0021*
IL-5	0.41 ± 0.07	0.02 ± 0.02	0.0061*
IL-6	736 ± 276.5	13.8 ± 4.2	0.0008†
IL-7	26.93 ± 3.59	9.68 ± 3.27	0.0646
IL-8	161.3 ± 65.95	16.78 ± 7.52	0.0045*
IL-9	28.87 ± 9.04	1.96 ± 1.01	0.0014*
IL-10	13.31 ± 2.79	0.44 ± 0.14	0.0008†
IL-12	33.10 ± 12.02	1.40 ± 1.23	0.0055*
IL-13	45.35 ± 8.74	5.67 ± 4.51	0.0251
IL-15	10.66 ± 1.46	2.68 ± 1.46	0.0257
IL-17	1.49 ± 0.49	0	0.3515
Eotaxin	3.77 ± 0.79	0.49 ± 0.36	0.1409
bFGF	5.98 ± 2.28	2.28 ± 2.28	0.8413
G-CSF	94.88 ± 13.57	7.20 ± 5.70	0.0055*
GM-CSF	130.9 ± 7.63	95.72 ± 10.1	0.088
IFN-γ	57.89 ± 8.69	0.98 ± 0.98	0.0008†
IP-10	58,249 ± 4564	163.5 ± 48.72	0.0008†
MCP-1	1556 ± 232	321.1 ± 48.9	0.0018*
MIP-1α	2.413 ± 0.56	0	0.052
MIP-1β	66.98 ± 9.89	6.06 ± 2.04	0.0008†
RANTES	71.21 ± 15.75	0.52 ± 0.52	0.0017*
TNF-α	17.69 ± 2,12	3.24 ± 1.62	0.0055*
VEGF	155.0 ± 99.59	18.88 ± 17.67	0.0190‡

* More significant difference ($P < 0.01$).
† Most significant difference ($P < 0.001$).
‡ Significant difference ($P < 0.025$).

Table 2. Serum Levels of 27 Types of Cytokines Determined by Using a Multiplex Bead Analysis System

	Sarcoidosis Vitreous, Mean ± SE ($N = 19$)	ERM Serum, Mean ± SE ($N = 5$)	*P* Value
PDGF-BB	8703 ± 511.7	8526 ± 1857	0.887
IL-1β	3.72 ± 0.58	5.91 ± 1.91	0.2268
IL-1ra	206.9 ± 22.42	223.3 ± 42.87	0.887
IL-2	5.12 ± 3.04	54.21 ± 49.40	0.721
IL-4	6.96 ± 1.25	5.76 ± 2.04	0.4342
IL-5	2.76 ± 0.23	25.99 ± 23.60	0.8868
IL-6	28.51 ± 10.50	116.1 ± 67.50	0.1355
IL-7	9.79 ± 0.89	8.12 ± 2.45	0.3935
IL-8	415.7 ± 193.3	791.3 ± 340.3	0.2554
IL-9	115.7 ± 51.05	59.81 ± 22.51	0.5695
IL-10	5.325 ± 0.91	5.43 ± 1.64	0.8869
IL-12	40.26 ± 6.12	83.49 ± 46.87	0.6698
IL-13	5.98 ± 1.59	7.79 ± 3.54	0.4772
IL-15	0	1.522 ± 1.27	0.0061*
IL-17	55.23 ± 8.65	48.43 ± 13.96	0.4339
Eotaxin	117.80 ± 18.12	117.0 ± 28.97	0.9433
bFGF	23.11 ± 5.93	43.42 ± 21.66	0.5426
G-CSF	28.46 ± 4.19	28.52 ± 8.69	1
GM-CSF	8.56 ± 2.67	77.93 ± 62.45	0.1803
IFN-γ	63.06 ± 7.97	124.9 ± 62.16	0.6187
IP-10	3485 ± 555.2	1053 ± 108.3	0.0105†
MCP-1	47.02 ± 10.83	64.83 ± 29.95	1
MIP-1α	68.39 ± 31.38	269.9 ± 161.6	0.1176
MIP-1β	752.7 ± 171.5	1777 ± 789.1	0.2007
RANTES	4318 ± 180.5	5077 ± 520.2	0.1768
TNF-α	52.21 ± 8.79	172.2 ± 76.81	0.0941
VEGF	103.9 ± 13.71	109.4 ± 30.01	0.9433

* More significant difference ($P < 0.01$).
† Significant difference ($P < 0.025$).

sarcoid control) patients. Interestingly, although the levels of these cytokines were much higher in vitreous fluid of patients with ocular sarcoidosis, the differences in the serum cytokine levels between these two groups (with only two exceptions) were not significant. Serum IP-10 was significantly higher in patients with ocular sarcoidosis than in those with ERM, but the serum levels of IL-15 were significantly lower than in patients with ERM.

The cytokine ratios of vitreous/serum in ocular sarcoidosis and ERM are shown in Table 3. The vitreous/serum ratios of PDGF-BB, IL-1ra, IL-4, IL-5, IL-6, IL-12, IL-13, G-CSF, IFN-γ, IP-10, MCP-1, MIP-1β, RANTES, TNF-α, and VEGF were significantly higher in ocular sarcoidosis samples than in those of ERM (nonsarcoid control) patients.

The Relationship between Postoperative Macular Thickness and Cytokine Concentrations

Data from the analysis of vitreous cytokines were compared with macular thickness 1 month after surgery (Fig.). Macular thickness in group 1 (10 patients and 12 eyes) was <359.5 μm, whereas measurements in group 2 (9 patients and 10 eyes) were ≥359.5 μm. The levels of most cytokines tend to increase in patients within the thin CME group. Notably, IL-1ra ($P = 0.02$), IL-2 ($P = 0.03$), IL-4 ($P = 0.03$), IL-8 ($P = 0.03$), IFN-γ ($P = 0.03$), IP-10 ($P = 0.01$), MCP-1 ($P = 0.03$), MIP-1β ($P = 0.005$), and RANTES ($P = 0.006$) were significantly upregulated in group 1. In contrast, the levels of PDGF-BB, IL-12, IL-13, bFGF, G-CSF, and VEGF seemed to be elevated in group 2 (no statistical difference).

Discussion

To the best of the authors' knowledge, this is the first study to investigate both vitreous and serum levels of cytokines, using multiplex ELISA analysis, in patients with ocular sarcoidosis. These patients had high levels of several types of cytokines, especially T helper 1 (Th-1)-related cytokines, in their vitreous body. In their investigation of the relationship between cytokine and clinical stage, the authors noticed that advanced pathologic stage in the posterior segment (e.g., complications such as severe CME) might be influenced by G-CSF, VEGF, and PDGF-BB, which are highly associated with vascular leakage, as previously reported.[29,30] In fact, only the cytokines that are associated with vascular permeability tended to undergo upregulation in the advanced CME stage. Previous reports have suggested that VEGF is strongly associated with blood-retina barrier (BRB) breakdown.[18] In contrast, almost all of the proinflammatory cytokines were downregulated in vitreous fluid from patients with advanced-stage ocular sarcoidosis (Fig.). It appears that numerous cytokines may be increased in order to increase the lymphocyte infiltration in vitreous fluid or macrophage infiltration into granulomas at the retinal layer. There is the potential for an increase in BRB breakdown from the high vitreous/serum ratio of cytokines, such as PDGF-BB, IL-6, G-CSF, and VEGF; if so, all inflammatory and angiogenic cytokine levels should increase in vitreous fluid after onset of

TABLE 3. Vitreous/Serum Ratio of 27 Types of Cytokines

	Sarcoidosis Vitreous/Serum, Mean ± SE ($N = 19$)	ERM Vitreous/Serum, Mean ± SE ($N = 5$)	*P* Value
PDGF-BB	0.006 ± 0.001	0.0001 ± 0.000009	0.0054*
IL-1β	0.61 ± 0.33	0.22 ± 0.20	0.0753 ns
IL-1ra	2.59 ± 1.26	0.03 ± 0.01	0.0022*
IL-2	4.45 ± 2.83	0	0.1470 ns
IL-4	0.39 ± 0.14	0.002 ± 0.002	0.0017*
IL-5	0.21 ± 0.03	0.01 ± 0.01	0.0096*
IL-6	90.69 ± 25.11	0.93 ± 0.72	0.0018*
IL-7	2.97 ± 0.59	1.91 ± 0.79	0.3555
IL-8	4.31 ± 1.29	0.09 ± 0.05	0.0229 ns
IL-9	1.54 ± 0.81	0.04 ± 0.03	0.0262 ns
IL-10	15.44 ± 8.79	4.49 ± 4.46	0.0283 ns
IL-12	1.12 ± 0.44	0.008 ± 0.005	0.0015*
IL-13	21.53 ± 8.94	0.53 ± 0.24	0.0129†
IL-15	Impossible to measure	0	Not measured
IL-17	0.36 ± 0.27	0	0.6944 ns
Eotaxin	0.36 ± 0.27	0	0.6944 ns
bFGF	0	0	ns
G-CSF	12.83 ± 5.06	0.27 ± 0.13	0.0028*
GM-CSF	21.86 ± 5.08	9.88 ± 7.57	0.1631 ns
IFN-γ	1.88 ± 0.61	0.02 ± 0.02	0.0008‡
IP-10	24.64 ± 3.86	0.13 ± 0.05	0.0008‡
MCP-1	58.14 ± 15.07	12.62 ± 5.51	0.0157†
MIP-1α	0.17 ± 0.05	0	0.0787
MIP-1β	0.20 ± 0.04	0.013 ± 0.01	0.0028*
RANTES	0.02 ± 0.004	0.0001 ± 0.0001	0.0017*
TNF-α	0.38 ± 0.09	0.03 ± 0.03	0.0017*
VEGF	0.81 ± 0.30	0.01 ± 0.007	0.0025*

ns, not specified.
* More significant difference ($P < 0.01$).
† Significant difference ($P < 0.025$).
‡ Most significant difference ($P < 0.001$).

the clinical condition. Moreover, the cytokine level in vitreous fluid for herpes virus or parasite infection, which might be associated with high BRB breakdown, was much higher than that for both nonocular sarcoidosis and ocular sarcoidosis. However, the number of groups studied is too limited to allow a comprehensive discussion for the present experiment. Further investigations should be performed to analyze the BRB breakdown, with comparison between blood and vitreous albumin concentration.

Interestingly, IP-10 was the only cytokine that was found to be elevated in both the vitreous body and serum of sarcoid uveitis patients. IP-10, also known as C-X-C motif chemokine 10, is a chemokine that is induced by IFN-γ and secreted from monocytes and macrophages stimulated with IFN-γ. Because IP-10 promotes the migration of T cells to sites of inflammation, it is an attractive candidate for further investigation of the mechanisms promoting the development of sarcoid granulomas. IP-10 is strongly expressed in sarcoid granuloma tissue,[26] and IP-10 secretion from alveolar macrophages is highly correlated with the $CD4^+$ T lymphocyte population. This finding may indicate that IP-10 secreted from macrophages in the granuloma tissue can regulate migration of $CD4^+$ T lymphocytes to the site of sarcoidosis during inflammatory processes in the posterior segment of the eye. The amount of $CD4^+$ T lymphocytes is related to IP-10 levels in BALF[26]; the authors observed a similar phenomenon in vitreous fluid samples in an ongoing experiment (manuscript submitted). The vitreous fluid from patients with ocular sarcoidosis had high amounts of $CD4^+$ T lymphocytes, but not $CD8^+$ T lymphocytes (data not shown; manuscript submitted). Reportedly, serum levels of IP-10 in patients with sarcoidosis were significantly higher than those of healthy volunteers; however, peripheral blood mononuclear cells did not increase the IP-10 production.[31] The present data indicated that IP-10 might be secreted from local macrophages that had infiltrated granuloma tissue in retina, vitreous fluid, or any other place in the body. In fact, the authors found that retinas from patients with sarcoid uveitis involved granulomas that contained $CD68^+$ macrophages (data not shown). Therefore, serum levels of IP-10 probably reflect the clinical state of sarcoid uveitis. High levels of Th-1-type cytokines in vitreous fluid suggest that IP-10 cooperates with Th-1-type cytokines, which act as local factors that promote T cell activation and proliferation.

Several cytokines have angiogenic/vascular permeability properties; for example, IL-6 increases vascular permeability.[32] Moreover, VEGF is a well-known angiogenic factor that is highly associated with vascular leakage in retinas of patients suffering with diabetic retinopathy, retinal vascular occlusion, or ROP. Vitreous levels of VEGF are significantly higher in eyes of patients with proliferative ROP than in those of control individuals, and VEGF is the only cytokine for which the vitreous level is correlated with vascular activity in ROP eyes.[33] Here, the authors intended to determine which cytokine(s) were correlated with critical clinical issues, such as the development of macular edema. The authors found that vitreous cytokines that are proangiogenic and/or associated with vascular leakage, such as VEGF, PDGF-BB, and G-CSF, tended to be upregulated in patients with severe macular edema (group 2), but not in patients with thin macular edema (group 1). In contrast, other proinflammatory and proangiogenic cytokines, such as MCP-1,[34] RANTES, IL-1ra,[35] and TNF-α,[36] which are all associated with vascular permeability, were downregulated in patients with severe macular edema. Moreover, IP-10, which has antiangiogenic properties, was significantly higher in the vitreous fluid of group 1 than in that of group 2. IP-10 prevents corneal hemangiogenesis[37] and inhibits growth and metastasis of lung carcinoma[38]; based on these findings, it is thought that high VEGF concentrations in vitreous fluids may be associated with macular edema and may enhance chronic inflammation. Furthermore, the balance of both proangiogenic and antiangiogenic cytokines was maintained until severe macular edema developed. Most patients in group 2 were treated with long-term steroids, or abandoned disease status before surgery. The visual acuity did not improve after surgery, most likely because of irreversible change of the sensory retina caused by long-standing macular edema (data not shown). Surprisingly, even in the patients who were treated with steroids before surgery, the vitreous fluid had higher cytokine levels than the vitreous fluid from the control group. The results suggest that proinflammatory cytokines that are upregulated in the vitreous fluid of ocular sarcoidosis patients might be influenced by BRB breakdown. It proved problematic to test for this in the present study because the limited amount of vitreous sample precluded comparison between serum and vitreous protein; however, VEGF, PDGF-BB, and G-CSF levels should be increased in primary status, not in the late stage of disease such as in group 2. Therefore, the authors believe that surgical intervention should be performed at an early stage of macular edema (before development of severe macular edema) for the purpose of removing proinflammatory cytokines from vitreous fluid.

Previous reports have shown that surgical intervention is beneficial for improvement of CME or ERM caused by sarcoid uveitis.[39,40] Here, the authors performed vitrectomy for acute-phase uveitis without CME or ERM. Diamond and Kaplan[41]

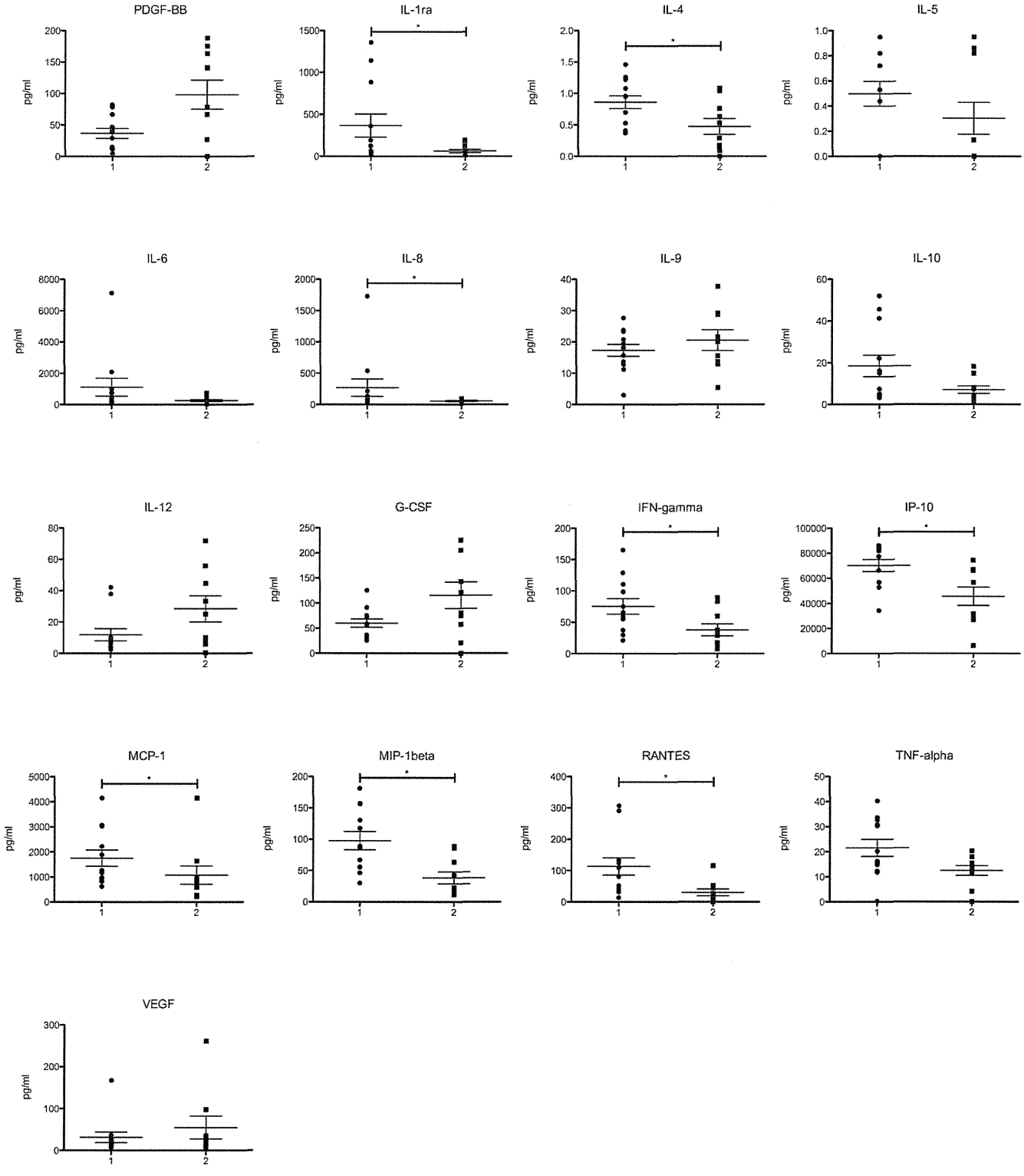

Figure. The relationship between postoperative macular thickness and cytokine concentration in vitreous fluid at 1 month after operation. The y-axis indicates the concentration of cytokines in vitreous fluid (pg/mL). The x-axis indicates the level of macular thickness. Patients were divided into two groups by macular thickness (average thickness of macular area [fovea 1000 μm across] ± DEV): thin CME range (1 = group 1) from 119.60 μm to 359.5 μm and thick CME range (2 = group 2) from 359.5 μm to 599.40 μm. Some patients overlapped because of different status of disease in each eye. $^*P < 0.05$.

have suggested that removal of inflammatory mediators (such as T cells) that accumulate in vitreous fluid in patients with uveitis may have a beneficial effect on macular edema. Likewise, the present study showed that removal of inflammatory cells and cytokines may lead to suppression of ocular inflammation. This report demonstrated that several proinflammatory cytokines persist at highly elevated levels in the vitreous fluid of patients with ocular sarcoidosis. Moreover, the authors confirmed that $CD4^+$ T cells also infiltrated into the vitreous fluid of patients with sarcoid uveitis (manuscript submitted).

The authors found that the retinal granulomas also had *P. acnes* DNA (data not shown). As with pulmonary sarcoidosis, the infectious theory should be considered for the etiology of ocular sarcoidosis. However, because the sample number was limited, further investigations and proper control samples are required to elucidate the role of *P. acnes* in ocular sarcoidosis. Therefore, eliminating the continuous exposure to proinflammatory cytokines, proinflammatory cells, and infectious agents (which were the key factors for inducing macular edema) by surgical intervention should be a beneficial treatment for preventing progression of uveitis. On the other hand, some anti-inflammatory cytokines, such as IL-4 and RANTES, were also upregulated in vitreous fluid in the present cases. These cytokines seemed to increase in moderate inflammatory status either to balance the Th1 and Th2 status, or to recruit the T regulatory cells for suppressing inflammation. Notably, RANTES is likely to be a key chemokine for suppressing inflammation in an experimental autoimmune uveitis model for recruiting anti-inflammatory $CD8^+$ T cells.[42] However, in this study, the number of vitreous $CD8^+$ T lymphocytes did not differ significantly in patients who had high RANTES level in vitreous fluid (data not shown). Because the number of patients was limited in this study, further studies are required to investigate and analyze the relationship between RANTES level and $CD8^+$ T lymphocytes in vitreous fluid.

The limitations of this study include the lack of an accurate control group and the variability in the duration of postoperative follow-up. In comparison, the level of IL-1β in the vitreous in infectious uveitis (153.24 ± 117.33 pg/mL) was significantly higher than in ocular sarcoidosis (0.60 ± 0.08 pg/mL; $P < 0.01$). However, no specific elevation of cytokine was found in ocular sarcoidosis. Further investigations should be performed to analyze the specific elevation of cytokine in ocular sarcoidosis. Despite this, these findings strongly suggest that highly elevated levels of proinflammatory cytokines are present in the vitreous fluid of patients with sarcoid uveitis, and that surgical intervention may be beneficial by removing excess proinflammatory cytokines from the vitreous fluid. Further investigations are warranted.

Acknowledgments

The authors thank Kentaro Kojima, Hideki Komori, and Toru Yasuhara for the helpful sample collections. Moreover, the authors thank Wendy Chao for editing and critical reading of this manuscript.

References

1. Baughman RP, Lower EE, du Bois RM. Sarcoidosis. *Lancet*. 2003;361:1111–1118.
2. Margolis R, Lowder CY. Sarcoidosis. *Curr Opin Ophthalmol*. 2007;18:470–475.
3. Nunes H, Bouvry D, Soler P, Valeyre D. Sarcoidosis. *Orphanet J Rare Dis*. 2007;2:46.
4. Wu JJ, Schiff KR. Sarcoidosis. *Am Fam Physician*. 2004;70:312–322.
5. Rothova A. Ocular involvement in sarcoidosis. *Br J Ophthalmol*. 2000;84:110–116.
6. Statement on sarcoidosis: Joint Statement of the American Thoracic Society (ATS), the European Respiratory Society (ERS) and the World Association of Sarcoidosis and Other Granulomatous Disorders (WASOG) adopted by the ATS Board of Directors and by the ERS Executive Committee, February 1999. *Am J Respir Crit Care Med*. 1999;160:736–755.
7. Hiraga Y. An epidemiological study of clustering of sarcoidosis cases [in Japanese]. *Nippon Rinsho*. 1994;52:1438–1442.
8. Hosoda Y, Hiraga Y, Odaka M, et al. A cooperative study of sarcoidosis in Asia and Africa: analytic epidemiology. *Ann N Y Acad Sci*. 1976;278:355–367.
9. McGrath DS, Goh N, Foley PJ, du Bois RM. Sarcoidosis: genes and microbes—soil or seed? *Sarcoidosis Vasc Diffuse Lung Dis*. 2001;18:149–164.
10. Ishige I, Usui Y, Takemura T, Eishi Y. Quantitative PCR of mycobacterial and propionibacterial DNA in lymph nodes of Japanese patients with sarcoidosis. *Lancet*. 1999;354:120–123.
11. Yasuhara T, Tada R, Nakano Y, et al. The presence of Propionibacterium spp. in the vitreous fluid of uveitis patients with sarcoidosis. *Acta Ophthalmol Scand*. 2005;83:364–369.
12. Lynch JP III, Sharma OP, Baughman RP. Extrapulmonary sarcoidosis. *Semin Respir Infect*. 1998;13:229–254.
13. Crick RP, Hoyle C, Smellie H. The eyes in sarcoidosis. *Br J Ophthalmol*. 1961;45:461–481.
14. Ohara K, Okubo A, Sasaki H, Kamata K. Intraocular manifestations of systemic sarcoidosis. *Jpn J Ophthalmol*. 1992;36:452–457.
15. Jabs DA, Johns CJ. Ocular involvement in chronic sarcoidosis. *Am J Ophthalmol*. 1986;102:297–301.
16. Bonfioli AA, Orefice F. Sarcoidosis. *Semin Ophthalmol*. 2005;20:177–182.
17. Herbort CP, Rao NA, Mochizuki M. International criteria for the diagnosis of ocular sarcoidosis: results of the first International Workshop On Ocular Sarcoidosis (IWOS). *Ocul Immunol Inflamm*. 2009;17:160–169.
18. Yoshimura T, Sonoda KH, Sugahara M, et al. Comprehensive analysis of inflammatory immune mediators in vitreoretinal diseases. *PLoS One*. 2009;4:e8158.
19. Kezuka T, Sakai J, Usui N, Streilein JW, Usui M. Evidence for antigen-specific immune deviation in patients with acute retinal necrosis. *Arch Ophthalmol*. 2001;119:1044–1049.
20. Sato T, Kusaka S, Shimojo H, Fujikado T. Simultaneous analyses of vitreous levels of 27 cytokines in eyes with retinopathy of prematurity. *Ophthalmology*. 2009;116:2165–2169.
21. de Boer JH, van Haren MA, de Vries-Knoppert WA, et al. Analysis of IL-6 levels in human vitreous fluid obtained from uveitis patients, patients with proliferative intraocular disorders and eye bank eyes. *Curr Eye Res*. 1992;11(suppl):181–186.
22. Ongkosuwito JV, Feron EJ, van Doornik CE, et al. Analysis of immunoregulatory cytokines in ocular fluid samples from patients with uveitis. *Invest Ophthalmol Vis Sci*. 1998;39:2659–2665.
23. Curnow SJ, Falciani F, Durrani OM, et al. Multiplex bead immunoassay analysis of aqueous humor reveals distinct cytokine profiles in uveitis. *Invest Ophthalmol Vis Sci*. 2005;46:4251–4259.
24. Banerjee S, Savant V, Scott RA, Curnow SJ, Wallace GR, Murray PI. Multiplex bead analysis of vitreous humor of patients with vitreoretinal disorders. *Invest Ophthalmol Vis Sci*. 2007;48:2203–2207.
25. Yoshimura T, Sonoda KH, Ohguro N, et al. Involvement of Th17 cells and the effect of anti-IL-6 therapy in autoimmune uveitis. *Rheumatology (Oxford)*. 2009;48:347–354.

26. Agostini C, Cassatella M, Zambello R, et al. Involvement of the IP-10 chemokine in sarcoid granulomatous reactions. *J Immunol.* 1998;161:6413–6420.
27. Sugita S, Shimizu N, Watanabe K, et al. Use of multiplex PCR and real-time PCR to detect human herpes virus genome in ocular fluids of patients with uveitis. *Br J Ophthalmol.* 2008; 92:928–932.
28. Miyanaga M, Sugita S, Shimizu N, et al. A significant association of viral loads with corneal endothelial cell damage in cytomegalovirus anterior uveitis. *Br J Ophthalmol.* 2010;94: 336–340.
29. Mishra BB, Poulter LW, Janossy G, James DG. The distribution of lymphoid and macrophage like cell subsets of sarcoid and Kveim granulomata: possible mechanism of negative PPD reaction in sarcoidosis. *Clin Exp Immunol.* 1983;54:705–715.
30. Yao H, Duan M, Buch S. Cocaine-mediated induction of platelet-derived growth factor: implication for increased vascular permeability. *Blood.* 2011;117:2538–2547.
31. Mishra BB, Poulter LW, Janossy G, Sherlock S, James DG. The Kveim-Siltzbach granuloma: a model for sarcoid granuloma formation. *Ann N Y Acad Sci.* 1986;465:164–175.
32. Funatsu H, Yamashita H, Ikeda T, Mimura T, Eguchi S, Hori S. Vitreous levels of interleukin-6 and vascular endothelial growth factor are related to diabetic macular edema. *Ophthalmology.* 2003;110:1690–1696.
33. Mizuki N, Ohno S, Sato T, et al. Microsatellite polymorphism between the tumor necrosis factor and HLA-B genes in Behcet's disease. *Hum Immunol.* 1995;43:129–135.
34. Papadia M, Herbort CP, Mochizuki M. Diagnosis of ocular sarcoidosis. *Ocul Immunol Inflamm.* 2010;18:432–441.
35. Ishihara M, Ishida T, Mizuki N, Inoko H, Ando H, Ohno S. Clinical features of sarcoidosis in relation to HLA distribution and HLA-DRB3 genotyping by PCR-RFLP. *Br J Ophthalmol.* 1995;79:322–325.
36. Rosenberg GA, Estrada EY, Dencoff JE, Stetler-Stevenson WG. Tumor necrosis factor-alpha-induced gelatinase B causes delayed opening of the blood-brain barrier: an expanded therapeutic window. *Brain Res.* 1995;703:151–155.
37. Proost P, Schutyser E, Menten P, et al. Amino-terminal truncation of CXCR3 agonists impairs receptor signaling and lymphocyte chemotaxis, while preserving antiangiogenic properties. *Blood.* 2001;98:3554–3561.
38. Arenberg DA, Kunkel SL, Polverini PJ, et al. Interferon-gamma-inducible protein 10 (IP-10) is an angiostatic factor that inhibits human non-small cell lung cancer (NSCLC) tumorigenesis and spontaneous metastases. *J Exp Med.* 1996;184: 981–992.
39. Kiryu J, Kita M, Tanabe T, et al. Pars plana vitrectomy for epiretinal membrane associated with sarcoidosis. *Jpn J Ophthalmol.* 2003;47:479–483.
40. Kiryu J, Kita M, Tanabe T, Yamashiro K, Miyamoto N, Ieki Y. Pars plana vitrectomy for cystoid macular edema secondary to sarcoid uveitis. *Ophthalmology.* 2001;108:1140–1144.
41. Diamond JG, Kaplan HJ. Lensectomy and vitrectomy for complicated cataract secondary to uveitis. *Arch Ophthalmol.* 1978;96:1798–1804.
42. Sonoda KH, Sasa Y, Qiao H, et al. Immunoregulatory role of ocular macrophages: the macrophages produce RANTES to suppress experimental autoimmune uveitis. *J Immunol.* 2003; 171:2652–2659.

whereas 33% (four out of 12 cases) of FNAB samples obtained with the standard 25G needle were non-diagnostic.

Our pilot study results are based solely upon trans-scleral FNAB approach and the study was not designed to evaluate complication rates. However, encouraged with our preliminary results, a study using trans-vitreal approach is planned. Such a study will also provide comparative data regarding complication rates. Our study results need to be verified independently in a larger number of patients.

David E Pelayes,[1] Jorge O Zárate,[2] Charles V Biscotti,[3] Arun D Singh[4]

[1]Department of Ophthalmology and Ophthalmic Research, Laboratory and Vision Sciences, University of Buenos Aires, Argentina; [2]Department of Pathology, University of Buenos Aires, Argentina; [3]Department of Anatomic Pathology, Cleveland Clinic Foundation, Cleveland, Ohio, USA; [4]Department of Ophthalmic Oncology, Cole Eye Institute, Cleveland Clinic Foundation, Cleveland, Ohio, USA

Correspondence to Dr Arun D Singh, Department of Ophthalmic Oncology, Cole Eye Institute (i3-129), Cleveland Clinic Foundation, 9500 Euclid Avenue, Cleveland, Ohio 44195, USA; singha@ccf.org

Contributors Each author is qualified as they: (1) contributed substantially to conception and design, acquisition of data, analysis and interpretation of data; (2) drafted the article and revised it critically for important intellectual content; and (3) approved the final version to be published.

Competing interests None.

Ethics approval Approval provided by the IRB.

Provenance and peer review Not commissioned; internally peer reviewed.

Published Online First 16 May 2012

Br J Ophthalmol 2012;**96**:1147–1148.
doi:10.1136/bjophthalmol-2012-301572

REFERENCES

1. **Singh AD,** Pelayes DE, Brainard JA, *et al*. History, indications, techniques and limitations. *Monogr Clin Cytol* 2012;**21**:1–9.
2. **Augsburger JJ,** Shields JA. Fine needle aspiration biopsy of solid intraocular tumors: indications, instrumentation and techniques. *Ophthalmic Surg* 1984;**15**:34–40.
3. **Shields JA,** Shields CL, Ehya H, *et al*. Fine-needle aspiration biopsy of suspected intraocular tumors. The 1992 Urwick Lecture. *Ophthalmology* 1993;**100**:1677–84.
4. **Eide N,** Walaas L. Fine-needle aspiration biopsy and other biopsies in suspected intraocular malignant disease: a review. *Acta Ophthalmol* 2009;**87**:588–601.
5. **Biscotti CV,** Singh AD. Uveal metastases. *Monogr Clin Cytol* 2012;**21**:17–30.
6. **Turell ME,** Tubbs RR, Biscotti CV, *et al*. Uveal melanoma: prognostication. *Monogr Clin Cytol* 2012;**21**:55–60.
7. **Midena E,** Segato T, Piermarocchi S, *et al*. Fine needle aspiration biopsy in ophthalmology. *Surv Ophthalmol* 1985;**29**:410–22.
8. **Char DH,** Kemlitz AE, Miller T. Intraocular biopsy. *Ophthalmol Clin North Am* 2005;**18**:177–85.
9. **Young TA,** Burgess BL, Rao NP, *et al*. Transscleral fine-needle aspiration biopsy of macula choroidal melanoma. *Am j ophthalmol* 2008;**145**:297–302.
10. **Cohen VM,** Dinakaran S, Parsons MA, *et al*. Transvitreal fine needle aspiration biopsy: the influence of intraocular lesion size on diagnostic biopsy result. *Eye (Lond)* 2001;**15**:143–7.

Expression of prostaglandin F receptor in scleral and subconjunctival tissue

Prostaglandin F2α ($PGF_{2\alpha}$) analogues eye drops are regarded as a first choice for the treatment of glaucoma. The hypotensive action of $PGF_{2\alpha}$ analogues is thought to be attributed to an increase in uveoscleral outflow.[1] However, the underlying mechanisms have yet to be well defined. The purpose of this present study was to examine prostaglandin F receptor (FP) localisation in ocular tissue.

All experiments were conducted in accordance with the principles set forth in the Declaration of Helsinki. The expression of FP was examined by X-gal staining in ocular tissues of FP knockout mice carrying the β-galactosidase gene at the FP loci ($Ptgfr^{-/-}$ mice)[2] and reverse transcription PCR of human conjuncitival and scleral fibroblasts (see supplementary methods, published online only).

First, FP localisation was examined using $Ptgfr^{-/-}$ mice in which the β-galactosidase gene was 'knocked-in' at the FP gene. In the $Ptgfr^{-/-}$ mice, X-gal staining of ocular tissue revealed positive signals in the sclera and subconjunctival tissue, but not the corneal tissue, and dense positive signals in the tarsal muscle of the eyelids (figure 1). The sclera under ciliary body also showed positive signals. However, no positive signals could be found in the corneal or conjunctival epithelium. X-gal staining of the ocular tissue did not reveal positive signals in wild-type mice (data not shown).

Next, reverse transcription PCR analyses were performed. The expected length of PCR products (887 bp) was obtained from cultured human scleral fibroblasts and cultured human conjunctival fibroblasts, but not conjunctival epithelium (figure 2).

We investigated FP localisation in ocular tissue and found that scleral and subconjunctival tissues expressed FP. FP expression of the sclera is consistent with the theory of the increase in uveoscleral outflow.

Previous studies have reported FP localisation in human ocular tissue by in-situ hybridisation[3] or by immunohistochemistry.[4] Using in-situ hybridisation, Mukhopadhyay and associates[3] reported the presence of high levels of FP receptor messenger RNA transcripts in the blood vessels of the iris, choroid and ciliary body, in which FP mRNA transcript was predominantly present in the circular muscle. As C57BL/6 mice have substantial pigment in the uvea, including the iris, choroid and ciliary body, we were unable to detect X-gal staining in these tissues. However, we did detect dense positive signals of X-gal staining in the tarsal muscle of eyelids. FP might possibly be expressed in smooth muscles. On the other hand, we could not find FP expression in the ocular surface epithelium, although the immunohistochemistry findings showed a strong expression of FP in the ocular surface epithelium. We also could not detect FP-specific mRNA in human conjunctival epithelial cells, while we could detect it in human conjunctival and scleral fibroblasts. So, it is true that FP expression in ocular surface epithelial cells is less than in conjunctival and scleral fibroblasts. Furthermore, FP expression in the fibroblast but not

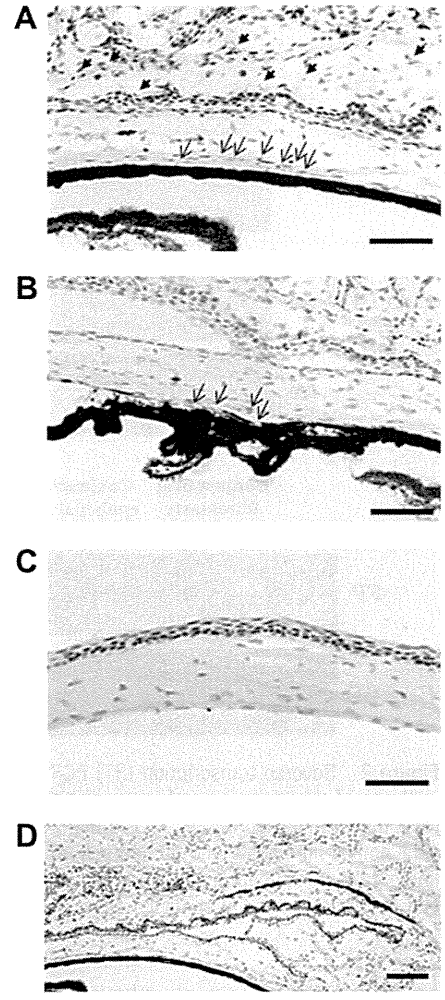

Figure 1 Histochemical staining for prostaglandin F receptor (FP) (X-gal). Ocular tissues from $Ptgfr^{-/-}$ mice expressing the β-galactosidase gene at the *Ptgfr* locus were stained for β-galactosidase activity with the substrate X-gal. Sections of ocular tissues from $Ptgfr^{-/-}$ mice were counterstained with haematoxylin (purple). Positive signals (blue) were shown on conjunctival fibroblasts (arrowhead: A), and sclera (arrow: A and B). (A) The backward sclera and conjunctiva; (B) ciliary body; (C) cornea; (D) tarsal muscle of the eyelid. Data are representative of three experiments (three $Ptgfr^{-/-}$ mice). Each bar represents a length of 100 μm.

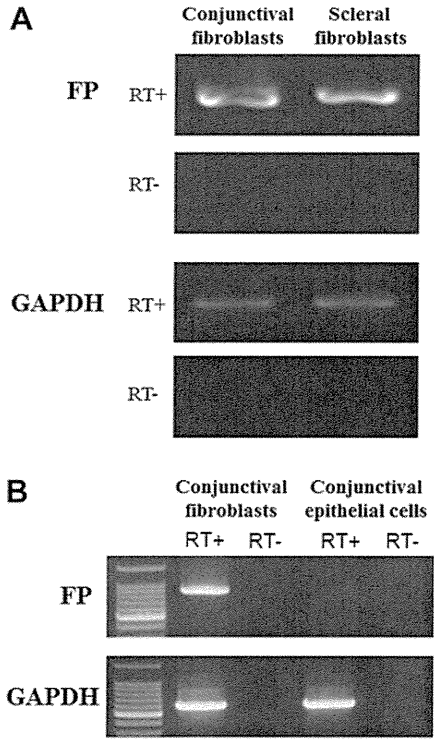

Figure 2 Reverse transcription (RT) PCR analyses of the expression of prostaglandin F receptor (FP)-specific mRNA. (A) Human conjunctival fibroblasts and human scleral fibroblasts; (B) human conjunctival fibroblasts and human conjunctival epithelial cells.

epithelial cells supports the theory of the increase in uveoscleral outflow.

Furthermore, it was also reported that $PGF_{2\alpha}$–FP signalling facilitates pulmonary fibrosis, and that $PGF_{2\alpha}$ could stimulate collagen production of lung fibroblasts via FP independently of transforming growth factor beta.[2] However, in cultured human conjunctival fibroblasts and scleral fibroblasts, transforming growth factor beta, but not $PGF_{2\alpha}$, could facilitate the collagen production in our experiment (data not shown), thus suggesting that $PGF_{2\alpha}$ analogues eye drops might not facilitate the fibrosis on the ocular surface.

In summary, the findings of this study showed that FP, the receptor of $PGF_{2\alpha}$, was expressed not only in the ciliary body, but also in scleral and subconjunctival tissues, suggesting that the $PGF_{2\alpha}$ analogues might affect not only the ciliary muscle but also the sclera and subcojunctiva.

Kojiro Imai,[1] Mayumi Ueta,[1,2] Kazuhiko Mori,[1] Morio Ueno,[1] Yoko Ikeda,[1] Toru Oga,[3] Norihiko Yokoi,[1] Katsuhiko Shinomiya,[1] Shuh Narumiya,[3] Shigeru Kinoshita[1]

[1]Department of Ophthalmology, Kyoto Prefectural University of Medicine, Kyoto, Japan; [2]Research Center for Inflammation and Regenerative Medicine, Faculty of Life and Medical Sciences, Doshisha University, Kyoto, Japan; [3]Department of Pharmacology, Graduate School of Medicine, Kyoto University, Kyoto, Japan

Correspondence to Dr Mayumi Ueta, Department of Ophthalmology, Kyoto Prefectural University of Medicine, 465 Kajii-cho, Hirokoji-agaru, Kawaramachi-dori, Kamigyo-ku, Kyoto 602-0841, Japan; mueta@koto.kpu-m.ac.jp

►An additional material is published online only. To view this file please visit the journal online (http://bjo.bmj.com/content/96/8.toc).

Contributors All authors made material contributions to this research. MU and KI were responsible for writing and reviewing contributions to the manuscript.

Competing interests None.

Ethics approval This study was approved by the Institutional Review Board of Kyoto Prefectural University of Medicine, Kyoto, Japan. All experimental procedures were conducted in accordance with the tenets set forth in the Declaration of Helsinki.

Provenance and peer review Not commissioned; internally peer reviewed.

Published Online First 11 May 2012

Br J Ophthalmol 2012;**96**:1148–1149. doi:10.1136/bjophthalmol-2012-301815

REFERENCES

1. **Nilsson SF,** Samuelsson M, Bill A, *et al*. Increased uveoscleral outflow as a possible mechanism of ocular hypotension caused by prostaglandin F2 alpha-1-isopropyl ester in the cynomolgus monkey. *Exp Eye Res* 1989;**48**:707–16.
2. **Oga T,** Matsuoka T, Yao C, *et al*. Prostaglandin F (2alpha) receptor signaling facilitates bleomycin-induced pulmonary fibrosis independently of transforming growth factor-beta. *Nat Med* 2009;**15**:1426–30.
3. **Mukhopadhyay P,** Bian L, Yin H, *et al*. Localization of EP(1) and FP receptors in human ocular tissues by in situ hybridization. *Invest Ophthalmol Vis Sci* 2001;**42**:424–8.
4. **Schlötzer-Schrehardt U,** Zenkel M, Nüsing RM. Expression and localization of FP and EP prostanoid receptor subtypes in human ocular tissues. *Invest Ophthalmol Vis Sci* 2002;**43**:1475–87.

Endothelial keratoplasty in children: surgical challenges and early outcomes

INTRODUCTION

A significant proportion of paediatric keratoplasties are performed for endothelial dysfunction due to failed graft, congenital hereditary endothelial dystrophy[1] and pseudophakic corneal oedema. Descemet's stripping endothelial keratoplasty (DSEK) is an evolving procedure for isolated endothelial dysfunction with encouraging results in adults. The application and outcome of this procedure in the paediatric population has not been well studied with few reports being published so far.[2–5]

This study reports the indications, surgical technique and early outcomes of DSEK in children <14 years of age.

METHODS

All children who underwent DSEK at our centre between January 2008 and January

Table 1 Preoperative and postoperative clinical data of children undergoing DSEK

Parameters	
Demographics	
Average age (in years)	8.06±3.95 years
Male:Female	3:1
Preoperative visual acuity	
Could not measure	8
<20/400	8
Indications for surgery	
Failed graft (PK performed for congenital hereditary endothelial dystrophy in five, microbial keratitis in two and corneal opacities in two cases; one case had a previous failed DSEK performed elsewhere for endothelial dysfunction following bee sting injury)	10 (62.5%)
Pseudophakic corneal oedema	3 (18.75%)
CHED	2 (12.5%)
Bee sting injury	1 (6.25%)
Surgical intervention	
Endothelial keratoplasty alone	15 (93.75%)
Endothelial keratoplasty + cataract surgery	1 (6.25%)
Follow-up	9.37±5.72 months
Average time for resolution of graft oedema	4.16±1.52 weeks (range 2–8 weeks)
Visual acuity at final follow-up	
Up to counting fingers 3 m	3 (18.75%)
20/400–20/100	8 (50%)
>20/80	5 (31.25%)
Complications	
Cataract in two cases (cataract surgery 2 months after DSEK)	
Glaucoma (Ahmed valve 6 months after DSEK) in one case	
Primary graft failure: one case	
Lenticule detachment in two cases: successful rebubbling in the postoperative period	

CHED, congenital hereditary endothelial dystrophy; DSEK, Descemet's stripping endothelial keratoplasty; PK, penetrating keratoplasty.

Expression of prostaglandin F receptor in scleral and subconjunctival tissue

Kojiro Imai, Mayumi Ueta, Kazuhiko Mori, et al.

Br J Ophthalmol 2012 96: 1148-1149 originally published online May 11, 2012
doi: 10.1136/bjophthalmol-2012-301815

Subfoveal Choroidal Thickness after Ranibizumab Therapy for Neovascular Age-related Macular Degeneration: 12-Month Results

Taizo Yamazaki, MD, Hideki Koizumi, MD, PhD, Tetsuya Yamagishi, MD, Shigeru Kinoshita, MD, PhD

Purpose: To investigate the changes in subfoveal choroidal thickness after intravitreal injections of ranibizumab (IVRs) for neovascular age-related macular degeneration (AMD).

Design: Prospective, consecutive, interventional case series.

Participants: Eighty eyes (40 affected eyes with neovascular AMD and 40 unaffected fellow eyes) of 40 patients.

Methods: Forty eyes with neovascular AMD were treated with 0.5-mg IVRs monthly for 3 months and received additional IVRs as needed over the following 9-month period. Subfoveal choroidal thickness in all 80 eyes was measured by use of enhanced depth imaging optical coherence tomography images before and after starting the IVRs.

Main Outcome Measures: Changes in subfoveal choroidal thickness after treatment by IVRs over a 12-month period.

Results: Twenty-three eyes (57.5%) were diagnosed with typical neovascular AMD, 16 eyes (40%) were diagnosed with polypoidal choroidal vasculopathy, and 1 eye (2.5%) was diagnosed with retinal angiomatous proliferation. Fifteen eyes (38%) had received some previous treatments for the neovascular lesion before undergoing the IVRs. The mean best-corrected visual acuity of the affected eyes was improved from 0.54 logarithm of the minimum angle of resolution units at baseline to 0.42 at 12 months ($P = 0.020$). The mean subfoveal choroidal thickness in the affected eyes decreased from 244±62 μm at baseline to 234±66 μm at 1 month ($P = 0.013$), 226±68 μm at 3 months ($P<0.001$), 229±67 μm at 6 months ($P = 0.002$), and 226±66 μm at 12 months ($P = 0.002$; the change ratio, 93%), whereas that in the unaffected eyes changed from 237±80 μm at baseline to 238±83 μm at 12 months ($P = 0.78$). In the affected eyes, the change ratio of subfoveal choroidal thickness at 12 months was not correlated with the number of IVRs (mean, 5.8±2.9). Subfoveal choroidal thickness demonstrated a similar trend toward decreasing during the following period independent of the subtypes of neovascular AMD or the treatment histories.

Conclusions: Subfoveal choroidal thickness decreased after IVRs in eyes with neovascular AMD. Intravitreal injections of ranibizumab may provide a pharmacologic effect not only on the neovascular lesion but also on the underlying choroid.

Financial Disclosure(s): The author(s) have no proprietary or commercial interest in any materials discussed in this article. *Ophthalmology 2012;119:1621–1627 © 2012 by the American Academy of Ophthalmology.*

Neovascular age-related macular degeneration (AMD) is a disorder associated with choroidal neovascularization (CNV) that frequently causes significant loss of vision.[1] Many kinds of therapies have been tried in an attempt to inhibit exudation induced by CNV. Ranibizumab (Lucentis; Genentech, South San Francisco, CA) is a humanized anti-vascular endothelial growth factor (VEGF) antibody fragment designed selectively to bind all forms of biologically active VEGF-A.[2,3] Intravitreal injection of ranibizumab (IVR) is currently a commonly used therapy for the treatment of neovascular AMD because IVR produces significant improvement of vision with low risks of serious systemic and ocular adverse events.[4–8] The efficacy and safety of IVR treatments have been reported for typical neovascular AMD, yet have also been reported for the other subtypes of neovascular AMD, namely, polypoidal choroidal vasculopathy (PCV)[9–13] and retinal angiomatous proliferation (RAP).[14–18]

Choroidal circulatory status seems to play an important role in the pathophysiology of neovascular AMD, for example, the findings of choroidal hypoperfusion were reportedly seen on indocyanine green angiography (ICGA) in eyes with neovascular AMD.[19–23] With regard to posttreatment hemodynamic changes in the choroid, photodynamic therapy (PDT) with verteporfin is known to induce temporary or permanent choroidal circulatory disturbances, as seen on ICGA.[24,25] However, the effect on the choroid induced by the therapeutic intervention of anti-VEGF medications has yet to be elucidated.

ISSN 0161-6420/12/$–see front matter
doi:10.1016/j.ophtha.2012.02.022

The imaging method known as enhanced depth imaging (EDI) optical coherence tomography (OCT) was recently introduced,[26] enabling clinicians to visualize the cross-sectional structure of the choroid. Several previous studies have reported successful measurements of the choroidal thickness using EDI OCT in normal eyes,[26,27] as well as in eyes with high myopia,[28] typical neovascular AMD,[29,30] PCV,[29–31] central serous chorioretinopathy,[32] Vogt–Koyanagi–Harada disease,[33] idiopathic macular hole,[34] and other disorders.[35–38]

Although IVR is widely understood to be effective for the resolution of pathologic fluid accumulation caused by CNV, little is known about the direct influences of IVR on the choroid under the CNV. In an attempt to assess the effect of IVR on the choroid in vivo, the current study investigated the changes in subfoveal choroidal thickness in eyes with neovascular AMD after IVRs over a 12-month period and compared them with those in the unaffected fellow eyes.

Patients and Methods

This prospective and interventional case series study involved 40 consecutive patients with neovascular AMD who were initially seen at the Macula Service of Kyoto Prefectural University of Medicine between March 2009 and May 2010. Each diagnosis of the subtype of neovascular AMD (typical neovascular AMD, PCV, and RAP) was based on the funduscopic and angiographic findings. Typical neovascular AMD was characterized by exudative changes due to CNV revealed by fluorescein angiography (FA) and ICGA. The diagnosis of PCV was based on ICGA findings, which demonstrated polypoidal structures at the border of the branching choroidal vascular networks.[39] In some cases, subpigment epithelial orange-red protrusions were biomicroscopically seen that corresponded to the polypoidal lesions revealed by ICGA. The diagnosis of RAP was based on the characteristic features, including intraretinal hemorrhage, intraretinal vascular anastomoses, and the OCT appearance of retinal pigment epithelial detachment with overlying cystic retinal edema.[40] Patients were excluded if their affected eyes had CNV secondary to other macular disorders, such as angioid streaks, or their fellow eyes had any macular disorder with visual loss. Patients were also excluded if each of the patients' eyes had any of the following criteria: (1) a spherical equivalent of −6 diopters (D) or less or chorioretinal atrophic changes secondary to pathologic myopia; (2) a history of intraocular surgery within 6 months; and (3) a history of pars plana vitrectomy. In addition, patients with systemic contraindication for IVRs were also excluded.

At baseline, all 40 patients underwent comprehensive ophthalmic examinations including refraction, best-corrected visual acuity (BCVA) testing with Landolt C charts, slit-lamp biomicroscopy with contact or noncontact lenses, color fundus photography, FA and ICGA using a confocal scanning laser ophthalmoscopy (Heidelberg Retina Angiograph II; Heidelberg Engineering Inc., Dossenheim, Germany), and a spectral-domain OCT (3D-OCT 1000 Mark II; Topcon Corporation, Tokyo, Japan). At each monthly visit over a 12-month period, all patients underwent BCVA testing, slit-lamp biomicroscopy, color fundus photography, and OCT imaging. The EDI-OCT images of the affected eyes with neovascular AMD were obtained at baseline, 1 month, 3 months, 6 months, and 12 months, and those of their unaffected fellow eyes were obtained at baseline and at 12 months as a control. Fluorescein angiography and ICGA were performed at 3 and 12 months and if deemed necessary.

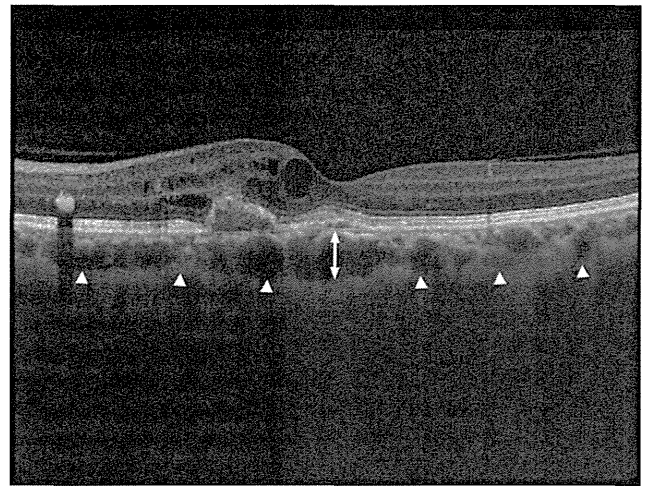

Figure 1. Enhanced depth imaging optical coherence tomography showing the retinal pigment epithelial detachment and the macular edema caused by polypoidal choroidal vasculopathy. *Double-headed arrow* indicates the subfoveal choroidal thickness. *Arrowheads* indicate the inner surface of the sclera.

The method used in the present study for obtaining the EDI OCT images was the same as reported previously.[26,29] Briefly, the choroid was imaged by positioning a spectral-domain OCT instrument close enough to the eye to obtain an inverted image. By means of the choroidal mode within the OCT that was used, the inverted images automatically appeared on the monitor to match those seen with the conventional imaging. The 6-mm horizontal and vertical scans, each comprising a maximum of 16 averaged scans, were obtained through the center of the fovea. Next, the 1 scan of 2 scans in which the inner surface of the sclera was more clearly visualized was selected. Subfoveal choroidal thickness was defined as the distance between the hyperreflective line corresponding to Bruch's membrane beneath the retinal pigment epithelium and the inner surface of the sclera by using the caliper function of the OCT device (Fig 1). The reliability of the choroidal thickness measurement method applied in the present study has been validated by the findings in our previous report.[29] All of the measurements were obtained by investigators who were masked to the patients' information.

All 40 patients were administered a 0.5-mg IVR monthly for 3 months: at baseline, at 1 month, and at 2 months. From 3 months onward, the patients received additional IVRs if any of the following criteria were observed: (1) persistent or recurrent subretinal or intraretinal fluid detected by OCT, (2) a new macular hemorrhage, (3) a new evolution of classic CNV, or (4) an expanding pigment epithelial detachment.

The primary outcomes were the changes in subfoveal choroidal thickness in the affected eyes treated with IVRs and those in the unaffected fellow eyes. The change ratio of subfoveal choroidal thickness at each time point to that at baseline was then calculated. When no change of subfoveal choroidal thickness was induced by IVRs, the change ratio was considered to be 100%.

The data obtained from all patients were analyzed with frequency and descriptive statistics. Mean values were compared by use of the Mann–Whitney *U* test or a Wilcoxon signed-rank test. The correlations between patient age or the spherical equivalent and subfoveal choroidal thickness, as well as the association between the change ratio of subfoveal choroidal thickness at 12 months and the number of IVRs administered, were assessed by use of the Spearman's rank correlation test. The differences in

outcomes among the neovascular lesions categorized by FA were compared by use of the Kruskal–Wallis test. The BCVA was converted to the logarithm of the minimum angle of resolution (logMAR) units before the calculations. Data were expressed as mean ± standard deviation, and a P value less than 0.05 was considered to be significant. All statistical analyses were performed with Statcell software version 1.0 (OMS Publishing Inc., Saitama, Japan). The study protocol followed the tenets of the Declaration of Helsinki and was approved by the institutional review board of Kyoto Prefectural University of Medicine.

Results

Eighty eyes (40 affected eyes with neovascular AMD and 40 unaffected fellow eyes) of 40 patients (16 female [40%] and 24 male [60%]; mean age: 70.7±7.7 years; range, 52–89 years) were evaluated in this study. Original refractive errors could not be identified for 6 affected eyes and 4 unaffected eyes that had undergone cataract surgery elsewhere more than 6 months before examination. Therefore, with the exception of pseudophakic eyes, the mean spherical equivalents of the remaining 34 affected eyes and 36 unaffected eyes were 0.13±1.44 D (range, −2.50 to 3.63 D) and 0.55±1.46 D (range, −2.63 to 3.50 D), respectively, with no significant difference (P = 0.16). Before the administration of the IVRs, 15 of the 40 affected eyes (38%) had received some previous treatment for neovascular lesion, including 1 to 2 sessions of PDT monotherapy (9 eyes), PDT combined with an intravitreal bevacizumab injection (IVB) (2 eyes), 1 to 2 sessions of IVB alone (3 eyes), and conventional laser photocoagulation (1 eye). At baseline, the neovascular lesions were categorized by FA as predominantly classic type (8 eyes, 20%), minimally classic type (10 eyes, 25%), and occult with no classic type (22 eyes, 55%). As to the subtypes of the neovascular lesions, 23 eyes (57.5%) were diagnosed with typical neovascular AMD, 16 eyes (40%) were diagnosed with PCV, and 1 eye (2.5%) was diagnosed with RAP. The mean number of IVRs that were administered over the 12-month period was 5.8±2.9 (range, 3–12).

The mean logMAR BCVA of the 40 affected eyes was 0.54 (median, 0; range, −0.08 to 2.00) at baseline, 0.50 (median, 0.46; range, −0.08 to 2.00) at 1 month, 0.45 (median, 0.40; range, −0.08 to 2.00) at 3 months, 0.42 (median, 0.40; range, −0.18 to 2.00) at 6 months, and 0.42 (median, 0.35; range, −0.08 to 1.40) at 12 months. Compared with that at baseline, the mean BCVA at 1 month, 3 months, 6 months, and 12 months were all significantly improved (P = 0.026, 0.006, 0.005, and 0.020, respectively). The mean logMAR BCVA of the unaffected eyes was 0.004 (median, 0.00; range, −0.18 to 0.70) at baseline.

Of the 40 affected eyes, the mean subfoveal choroidal thickness as measured by use of the obtained EDI-OCT images was significantly reduced from 244±62 μm at baseline to 234±66 μm (change ratio compared with baseline, 96%) at 1 month (P = 0.013), 226±68 μm (92%) at 3 months (P<0.001), 229±67 μm (94%) at 6 months (P = 0.002), and 226±66 μm (93%) at 12 months (P = 0.002) (Fig 2), whereas that of the 40 unaffected eyes was basically unchanged from 237±80 μm at baseline to 238±83 μm (100%) at 12 months (P = 0.78). Subfoveal choroidal thickness of the affected eyes at baseline was not correlated with patient age and spherical equivalent (rs = −0.005, P = 0.97, and rs = 0.31, P = 0.069, respectively). In addition, subfoveal choroidal thickness of the unaffected eyes at baseline was not correlated with age or spherical equivalent (rs = −0.055, P = 0.73, and rs = 0.31, P = 0.070, respectively). In the affected eyes, the change ratio of subfoveal choroidal thickness at 12 months to that at baseline was not correlated with the number of IVRs administered over the 12-month period (rs = 0.15, P = 0.42).

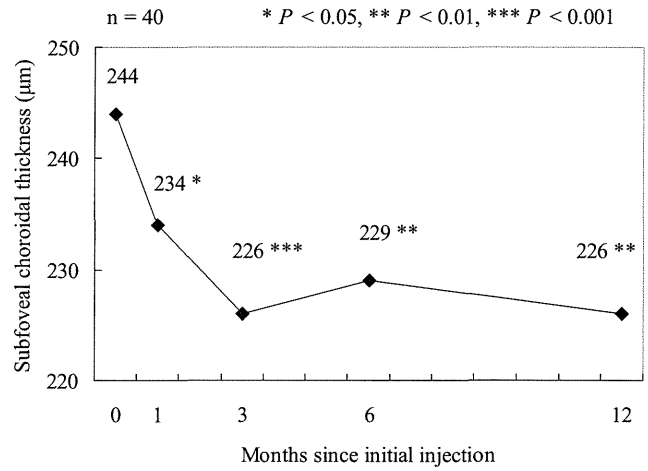

Figure 2. Changes in the mean subfoveal choroidal thickness in 40 eyes with neovascular age-related macular degeneration over the 12-month period after the initial intravitreal injections of ranibizumab. The mean subfoveal choroidal thickness significantly decreased at 1, 3, 6, and 12 months compared with baseline (0).

In regard to the subtypes of neovascular AMD, the mean subfoveal choroidal thickness at baseline was 235±65 μm in 23 eyes with typical neovascular AMD and 261±54 μm in 16 eyes with PCV. However, the difference between the 2 subtypes was not significant (P = 0.21). After starting IVRs, subfoveal choroidal thickness in eyes with typical neovascular AMD and in eyes with PCV demonstrated a similar trend toward decreasing over the following 12-month period. The mean subfoveal choroidal thickness in eyes with typical neovascular AMD was 229±72 μm (change ratio compared with baseline, 97%) at 1 month, 215±73 μm (90%) at 3 months, 220±68 μm (93%) at 6 months, and 218±65 μm (93%) at 12 months. Compared with baseline, the mean subfoveal choroidal thickness at 3 months, 6 months, and 12 months was significantly reduced (P = 0.005, 0.007, and 0.007, respectively). The mean subfoveal choroidal thickness in 16 eyes with PCV was 245±57 μm (94%) at 1 month, 246±56 μm (95%) at 3 months, 247±64 μm (95%) at 6 months, and 243±68 μm (93%) at 12 months. Compared with baseline, the mean subfoveal choroidal thickness significantly decreased at 1 month (P = 0.028) and 3 months (P = 0.047). In 1 eye with RAP that had previously received PDT combined with an IVB, subfoveal choroidal thickness was 177 μm at baseline and decreased to 163 μm (92%) at 1 month, 159 μm (90%) at 3 months, 157 μm (89%) at 6 months, and 159 μm (90%) at 12 months. These results are summarized in Figure 3.

The mean subfoveal choroidal thickness at baseline was 245±66 μm in 25 eyes without previous treatments and 242±56 μm in 15 eyes with previous treatments, with no significant difference found between the 2 groups (P = 0.75). The mean subfoveal choroidal thickness of those 2 groups demonstrated a similar trend toward decreasing over the following 12-month period. The mean subfoveal choroidal thickness in eyes without previous treatments was 233±74 μm (change ratio compared with baseline, 94%) at 1 month, 227±76 μm (92%) at 3 months, 228±73 μm (93%) at 6 months, and 229±71 μm (93%) at 12 months. Compared with baseline, the mean subfoveal choroidal thickness at all 4 time points was significantly reduced (P = 0.038, 0.013, 0.008, and 0.024, respectively). The mean subfoveal choroidal thickness in eyes with previous treatments was 235±52 μm (98%) at 1 month, 223±54 μm (93%) at 3 months, 230±59 μm (95%) at 6 months, and 222±59 μm (92%) at 12 months. Compared with

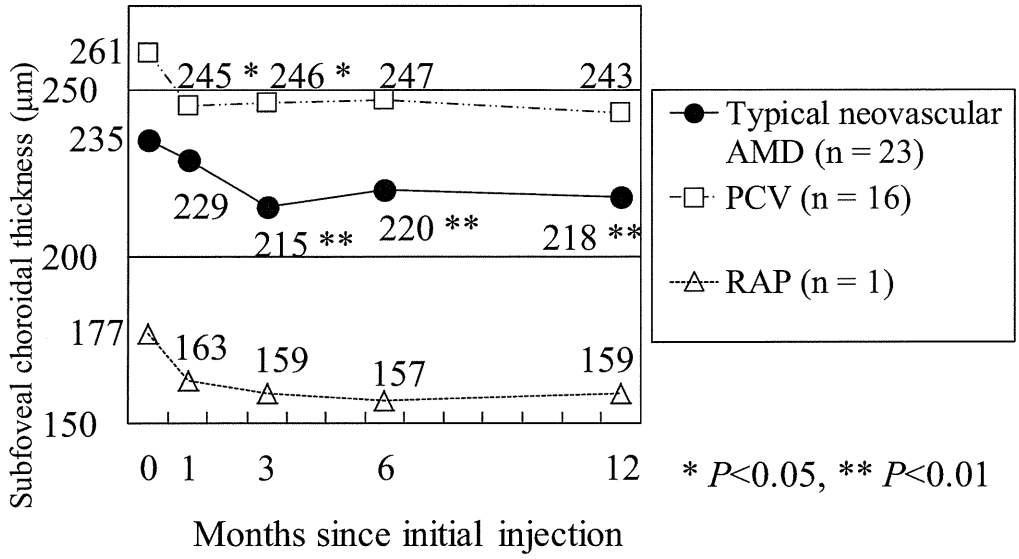

Figure 3. Changes in the mean subfoveal choroidal thickness in eyes with typical neovascular age-related macular degeneration (AMD), polypoidal choroidal vasculopathy (PCV), and retinal angiomatous proliferation (RAP) over the 12-month period after the initial intravitreal injections of ranibizumab. The subfoveal choroidal thickness in the 3 subtypes demonstrated a similar trend toward decreasing during the 12-month period. The mean subfoveal choroidal thickness in eyes with typical neovascular AMD at 3, 6, and 12 months significantly decreased compared with that at baseline (0). The mean subfoveal choroidal thickness in eyes with PCV was significantly reduced at 1 and 3 months compared with that at baseline.

baseline, the mean subfoveal choroidal thickness at 3 months and 12 months was significantly reduced (P = 0.013 and 0.023, respectively). These results are summarized in Figure 4. None of the 40 patients developed severe systemic or ocular complications related to IVRs.

Discussion

To the best of our knowledge, the changes in choroidal thickness during IVR therapy have not been reported. This is the first study to show the decreased subfoveal choroidal thickness in eyes with neovascular AMD treated with IVRs.

The mean subfoveal choroidal thickness in all 40 eyes treated with IVRs decreased from 244 μm at baseline to 226 μm at 3 months, which remained until 12 months. The rate of decrease in subfoveal choroidal thickness was 18 μm/year. The rate was greater than that reported in normal eyes (1.56 μm/year),[27] and results of the present study indicate the possibility that IVRs influenced the choroidal structure under the neovascular membrane in neovascular AMD. The

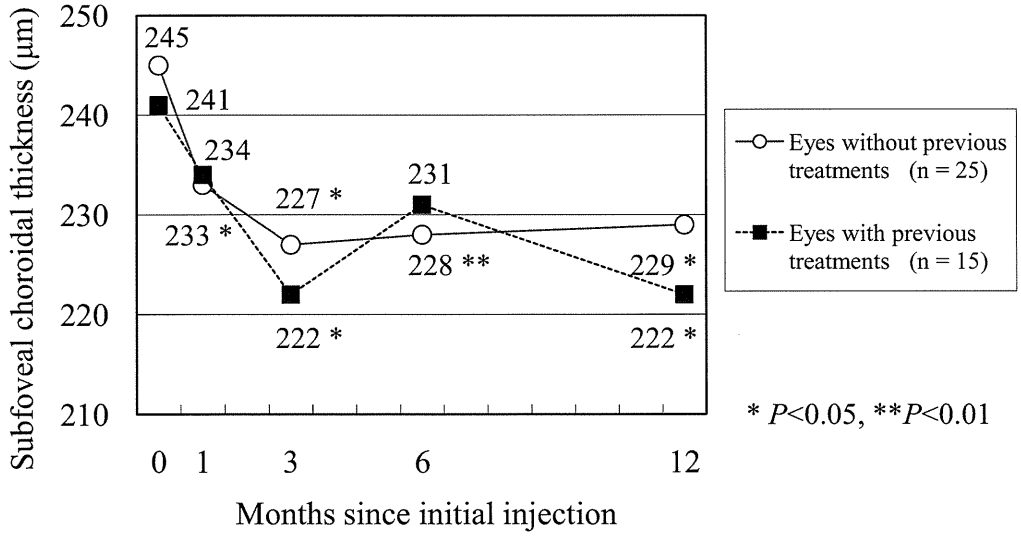

Figure 4. Change in the subfoveal choroidal thickness in eyes with or without previous treatments for neovascular age-related macular degeneration over the 12-month period after the initial intravitreal injections of ranibizumab. The mean subfoveal choroidal thickness in the 2 groups demonstrated a similar trend toward decreasing during the 12-month period. The mean subfoveal choroidal thickness in eyes without previous treatments significantly decreased at all 4 time points compared with that at baseline. The mean subfoveal choroidal thickness in eyes with previous treatments significantly decreased at 3 and 12 months compared with that at baseline (0).

mean subfoveal choroidal thickness after IVRs significantly decreased at 1 month and reached the maximum amount of decrease at 3 months. This trend might implicate that 1 injected dose of ranibizumab (0.5 mg) was sufficient to cause the significant decrease in choroidal thickness and that the additional 2 monthly administrations of IVRs had an additive effect. However, the correlation between the number of IVRs administered over the 12-month period and the change ratio of subfoveal choroidal thickness was not significant. Therefore, the findings of this study indicate that 3 monthly injections of IVRs were sufficient for the choroidal thickness to reach the maximum amount of decrease at 3 months that plateaued and remained unchanged independently of the number of additional IVRs.

Maruko and associates[31] recently reported that in both the PDT monotherapy and the combined therapy of PDT and IVR for PCV, subfoveal choroidal thickness transiently increased 2 days after PDT, followed by its significant decrease through 6 months. However, the authors did not comment on the additional effect of IVRs on the changes in subfoveal choroidal thickness. The analyses of data presented in their report revealed that the mean subfoveal choroidal thickness in 11 patients treated with combined therapy had slightly decreased from 264 μm to 262 μm in 1 or 2 days after IVR that preceded PDT.[31] In the current study, subfoveal choroidal thickness in eyes with PCV significantly decreased from 261 μm at baseline to 245 μm at 1 month and remained unchanged over 12 months. Our data may suggest that not only PDT but also IVRs may have an effect to decrease the choroidal thickness in eyes with PCV, although the rate of the reduction induced by IVR alone seemed to be less than that by PDT.[31] The difference in the degree of choroidal thickness decrease between PDT and IVR might be attributable to the different action mechanisms between these 2 treatments because PDT reportedly induces photothrombotic choroidal vascular occlusion.[24,25]

Recent studies have reported that eyes with PCV have a thicker choroid under the fovea than those with typical neovascular AMD.[29,30] In the present study, subfoveal choroidal thickness in eyes with PCV at baseline was not significantly thicker than that in eyes with typical neovascular AMD, possibly because of the influence on the choroid by the various previous treatments for the 7 eyes with typical AMD and the 7 eyes with PCV. Subfoveal choroidal thickness in eyes with the 3 subtypes of neovascular AMD, namely, typical neovascular AMD, PCV, and RAP, showed a similar trend toward decreasing during the following 12-month period, which may implicate that IVR has a constant effect on the choroid, regardless of the subtype of neovascular AMD and the treatment histories.

Vascular endothelial growth factor-A provides various pharmacologic actions on the choroid, such as increases in microvascular permeability, angiogenesis, and survival for the vascular endothelial cells.[2,3] Vascular endothelial growth factor-A is also considered to play a key role in the pathogenesis of neovascular AMD. In fact, a significantly increased expression of VEGF was measured in the aqueous humor of eyes with neovascular AMD, and a significant decrease of VEGF was observed after IVRs.[41] In rabbits, ranibizumab rapidly penetrates after intravitreal injection through all retinal layers to reach the choroid[42] and may have the potential to inhibit the activity of all VEGF-A isoforms.[2,3] One reason for the decreased choroidal thickness in the current study might be related to the reduction of choroidal vascular permeability, as seen in eyes with central serous chorioretinopathy treated with IVBs.[43] However, we were not able to draw a conclusion on the other reasons, such as morphologic changes in the choroidal vasculature itself, because to date it remains unclear whether IVR has a potential to provide a vasoconstriction effect on the choroidal vasculature similar to that reportedly seen in the retinal vasculature.[44,45] Further investigation on the cross-sectional choroidal structure using higher-resolution instruments may elucidate the reason why the choroidal thickness in neovascular AMD decreases after IVRs.

Study Limitations

The current study has several limitations, such as the limited number of cases that were included. The subfoveal choroidal thickness was investigated at the fixed time points; however, the relationship between subfoveal choroidal thickness and the disease activities still remains unknown. Although the measurements were performed by investigators masked to the patients' information, those measurements were performed manually. Future studies with automated software will be required for a more objective evaluation.

In conclusion, subfoveal choroidal thickness appeared to decrease after IVRs in eyes with neovascular AMD. Intravitreal injections of ranibizumab may provide a pharmacologic effect not only on the CNV but also on the choroid under the neovascular lesion. It may be intriguing to investigate which other anti-VEGF medications have a similar effect on the choroidal thickness to further understand their pharmacokinetics and the pathophysiology of neovascular AMD.

References

1. Wong TY, Chakravarthy U, Klein R, et al. The natural history and prognosis of neovascular age-related macular degeneration: a systematic review of the literature and meta-analysis. Ophthalmology 2008;115:116–26.
2. Lowe J, Araujo J, Yang J, et al. Ranibizumab inhibits multiple forms of biologically active vascular endothelial growth factor in vitro and in vivo. Exp Eye Res 2007;85:425–30.
3. Ferrara N, Damico L, Shams N, et al. Development of ranibizumab, an anti-vascular endothelial growth factor antigen binding fragment, as therapy for neovascular age-related macular degeneration. Retina 2006;26:859–70.
4. Mitchell P, Korobelnik JF, Lanzetta P, et al. Ranibizumab (Lucentis) in neovascular age-related macular degeneration: evidence from clinical trials. Br J Ophthalmol 2010;94:2–13.
5. Brown DM, Kaiser PK, Michels M, et al, ANCHOR Study Group. Ranibizumab versus verteporfin for neovascular age-related macular degeneration. N Engl J Med 2006;355:1432–44.
6. Rosenfeld PJ, Brown DM, Heier JS, et al, MARINA Study Group. Ranibizumab for neovascular age-related macular degeneration. N Engl J Med 2006;355:1419–31.